Eur. Phys. J. C (2022) 82:473
https://doi.org/10.1140/epjc/s10052-022-10413-x

THE EUROPEAN PHYSICAL JOURNAL C

Regular Article - Theoretical Physics

Semileptonic D meson decays to the vector, axial vector and scalar mesons in Hard-Wall AdS/QCD correspondence

S. Momeni[1,a], **M. Saghebfar**[1,2,b]

[1] Department of Electrical Engineering, Shahid Beheshti University, Tehran, Iran
[2] Optics-Laser Science and Technology Research Center, Malek Ashtar University of Technology, Isfahan, Iran

Received: 9 October 2021 / Accepted: 10 May 2022 / Published online: 23 May 2022

Abstract In this work, a Hard-Wall AdS/QCD model with 4 flavours is utilized to calculate the transition form factors for the semileptonic $D \to (V, A, S)\,\ell\,\nu_\ell$. These decays occur by $c \to d\,\ell\,\nu_\ell$ transition at quark level for $D^0 \to \rho^-(b_1^-, a_1^-, a_0^-)\,\ell\,\nu_\ell$, $D_s^+ \to K_0(K_{1A}^0, K_{1B}^0)\,\ell\,\nu_\ell$ decays while the semileptonic decays $D^0 \to K^{*-}(K_{1A}^-, K_{1B}^-, K_0^-)\,\ell\,\nu_\ell$ and $D^+ \to \bar{K}_0(\bar{K}_{1A}^0, \bar{K}_{1B}^0)\,\ell\,\nu_\ell$ proceed by $c \to s\,\ell\,\nu_\ell$ transition. The masses and decay constants of scalar mesons as well as the form factors and the branching ratios of aforementioned decays are calculated in our model, and a comparison is also made between our results and predictions of other theoretical methods and the existing experimental values.

1 Introduction

Charm mesons are the lightest particles involve a c quark therefore, their decays are good tools for the study of the weak interactions. In recent years, experimental development has been achieved in considering semileptonic decays of these groups of mesons. The most valuable measurements are reported from BES III. In this collaboration analysis are presented for $D^+ \to \bar{K}^0\,e^+\,\nu_e$, $D^+ \to \pi^0\,e^+\,\nu_e$, $D^{0(+)} \to \pi^{-(0)}\,\mu^+\,\nu_\mu$, $D_s^+ \to \phi\,e^+(\mu^+)\,\nu_{e(\mu)}$, $D_s^+ \to \eta(\eta')\,\mu^+\,\nu_\mu$, $D^+ \to \eta(\eta')\,e^+\,\nu_e$, $D^0 \to K^-\,\mu^+\,\nu_\mu$, $D_s^+ \to K^{0(*0)}\,e^+\,\nu_e$, $D^0 \to \bar{K}^0\,\pi^-\,e^+\,\nu_e$, $D^+ \to f_0(500)\,e^+\,\nu_e$ and $D \to \rho\,e^+\,\nu_e$ decays [1–9]. In addition, the data extracted from Belle II collaboration are used to evaluate important observable for $D_s^{*+} \to D_s^+\,\gamma$, $D_s^+ \to \mu^+(\tau^+)\,\nu_{\mu(\tau)}$, $D^{*+} \to D^0\,\pi^+$, $D^0 \to K^-(\pi^-)\,\ell^+\nu_\ell$ and $D^0 \to \nu_\ell\bar{\nu}_\ell$ decays [10–12]. On the other hand, Theoretical Studies of D mesons semileptonic decays are helpful tools to:

- Consider non-perturbative aspects of hadronic physics, since charmed mesons masses $\mathcal{O}(2\,\text{GeV})$ are small enough to apply our studies in this region.
- Estimate elements of the Cabibbo-Kobayashi-Maskawa (CKM) matrix.
- Analysis leptonic decay constants of the initial and final meson states.
- Check the standard model (SM) implying the lattice QCD simulations to the charmed hadron data.
- Probe the new physics (NP) beyond the SM considering background-free low-energy signals provided in charmed meson transitions.

The first step in studying hadronic decays is to evaluate form factors, which can give an overview from distribution of hadronic matter and the strong interaction between particles involved in the transition. The form factors are functions of q^2 where q is the transfer momentum. Having form factors, theoretical predictions for many observable such as branching fraction, CP asymmetry, Isospin asymmetry and Forward–Backward asymmetry can be done. D meson transitions are studied via different approaches. The covariant confined quark model (CCQM) framework is utilized to evaluate form factors of $D^+ \to (D^0, \rho^0, \omega, \eta, \eta')\ell^+\nu$ and $D_s^+ \to (D^0, \phi, K^0, K^{*0}, \eta, \eta')\ell^+\nu$ decays in [13,14]. The form factors of $D \to \pi(K, \rho)\,\ell\,\nu$ decays are estimated via Light-Cone QCD Sum Rules (LCSR) approach in [15–18]. In the LCSR method, operator product expansions (OPE) on the light-cone are combined with QCD sum rule techniques in the region where q^2 is near zero. In [19], the experimental measurements are used to determine the form factors of $D \to K\ell\nu$ transition. The semileptonic processes $D \to \pi, \rho, K$ and K^* have been investigated by the heavy quark effective theory (HQET) in Ref. [20], and the form factors of the $D \to \pi(K, K^*)\ell\,\nu$ decays have been calculated by the lattice QCD (LQCD) approach in Refs. [21–23]. The LQCD can be used to determine the form factors in

[a] e-mail: samira.momeni@ph.iut.ac.ir (corresponding author)
[b] e-mail: saghebfar@mut-es.ac.ir

a limited range of q^2 ($q^2 \to q^2_{max}$). The three-point QCD sum rules (3PSR) framework have been used to consider the semileptonic decays $D_{(s)} \to f_0(K_0^*)\,\ell\,\nu$, $D_{(s)} \to \pi(K)\,\ell\,\nu$, $D_{(s)} \to K^*(\rho,\phi)\,\ell\,\nu$ $D_q \to K_1\,\ell\,\nu\,(q = u,d,s)$ and $D \to a_1$, $f_1(1285)$, $f_1(1420)$ in [24–34]. The gauge/gravity correspondence approach, which is inspired from the relation between a type IIB string theory and super Yang–Mills theory in the large N_c limit with $\mathcal{N} = 4$ [35–37], has been used to study both gravitational and gauge parts in recent years. The anti-de Sitter space/quantum chromodynamics correspondence is developed in 2 ways:

- (AdS/LF QCD): In this approach, the QCD theory is written in light-front (LF) coordinate and the Schrödinger-like wave function equation for a hadron in this coordinate, can be mapped to the equation of motion that describes the hadrons in the AdS space. The light-front distribution amplitudes (DAs) are derived from the holographic light-front wave functions (LFWFs); more information is given in [38–43]). This model is utilized to evaluate DAs of vector, axial vector and pseudoscalar mesons and study B meson decays, Electro magnetic form factors and parton distribution functions (TDMs) in [44–55].
- (AdS/QCD): In this model, used in this paper, corresponding to every field in the gravitational AdS_5 space, an operator is defined in 4-dimensional gauge theory. The hadronic form factors and strong coupling can be obtained via a connection between the correlation functions involving n currents and the functional differentiation from the 5D action with respect to their n sources. The masses, electromagnetic and gravitational form factors of mesons, $K_{\ell 3}$ transition form factors, the strong couplings $g_{\rho^n\rho\rho}$, $g_{\rho^n KK}$, $g_{\rho^n K^*K^*}$, $g_{\rho^n DD}$ and $g_{\rho^n D^*D^*}$ are estimated via this framework in [56–62,64**?** –67]. Moreover, $(D^{(*)}, D, A)$, $(D^{(*)}, D^{(*)}, V)$, (D_1, D_1, P), $(\psi, D, D^{(*)}, P)$ and $(\psi, D, D^{(*)}, A)$ vertices are analyzed using this model in [68].

The main purpose of this paper is the form factor investigation for the semileptonic $D \to (V,A,S)\,\ell\,\nu_\ell$ decays with $D = (D^0, D^+, D_s^+)$, $V = (\rho^-, K^{*-})$, $A = (a_1^-, b_1^-, K_1^-, K_1^0, \bar{K}_1^0)$, $S = (a_0^-, K_0^-, K_0, \bar{K}_0)$ and $\ell = e, \mu$, in a Hard-Wall AdS/QCD model with $N_f = 4$. In the model that is used in this study, we can predict the form factors of charm meson decays in all of the physical range of q^2, which is an advantage of the AdS/QCD model in studying charm meson decays. This paper is organized as follows: the presented model, including scalar, pseudoscalar, vector and axial vector mesons, is introduced in Sect. 2. The wave functions and the decay constant of aforementioned mesons are also extracted from the model in this section. The form factors for the semileptonic decays of $D \to (V,A,S)\,\ell\,\nu_\ell$ are derived in Sect. 3., and the numerical analysis for the masses and wave functions of mesons as well as the form factors and branching ratios for considered semileptonic decays are described in Sect. 4. For a better analysis, a comparison is made between our estimations and the results of other methods and existing experimental values. Finally, Sect. 5 is reserved for our conclusion and discussions.

2 The Hard-Wall AdS/QCD model involving scalar, pseudoscalar, vector and axial vector mesons: wave functions, decay constant and masses

The first step, in our framework, to evaluate form factors or strong couplings is to estimate wave functions in 5 dimensions for the mesons included in the model. For this aim, the Anti-de Sitter space metric is chosen as:

$$ds^2 = g_{MN}\,dx^M\,dx^N = \frac{R^2}{z^2}\,\eta_{MN} dx^M\,dx^N, \tag{1}$$

where $M,N = 0,1,2,3,4$ and $\eta_{MN} = \text{diag}(1,-1,-1,-1,-1)$. Moreover, the warp factor is shown with R, which can be chosen as $R = 1$ in pure AdS [69]. In Hard-Wall AdS/QCD, the AdS space is compactified by two different boundary conditions on radial coordinate z. The UV boundary at $z = \varepsilon \to 0$ corresponds to the UV limit of QCD, and the conformal symmetry of QCD is broken by locating a wall at $z = z_m$, which also simulates the confinement feature of QCD. According to the general philosophy of the AdS/QCD, every operator in the 4D field theory corresponds to a 5D source field in bulk. Here, the correspondences are:

$$\begin{aligned} L^{\mu,a} &\leftrightarrow J_L^{\mu,a} = \bar{q}_L\,\gamma^\mu\,t^a\,q_L, \\ R^{\mu,a} &\leftrightarrow J_R^{\mu,a} = \bar{q}_R\,\gamma^\mu\,t^a\,q_R, \\ X &\leftrightarrow \bar{q}_L\,q_R, \end{aligned} \tag{2}$$

where $L(R)^{\mu,a}$, X and q are the N_f left-handed (right-handed) gauge, scalar and quark field, respectively. Moreover, $q_{L/R} = (1 \pm \gamma_5)\,q$ and for $SU(N_f)$ group t^a (with $a = 1,\ldots N_f^2 - 1$) are the generators by the trace condition $\text{Tr}(t^a\,t^b) = 1/2\,\delta^{ab}$. In this paper, the 5D action with $SU(N_f)_L \otimes SU(N_f)_R$ symmetry is considered as [69]:

$$\begin{aligned} S = \int d^5x\,\sqrt{g}\,\text{Tr}\Big\{ &(D_M X)\,(D^M X)^\dagger + 3\,|X|^2 \\ &- \frac{1}{4g_5^2}\left(L^{MN}\,L_{MN} + R^{MN}\,R_{MN}\right)\Big\}, \end{aligned} \tag{3}$$

where the field strengths are defined by:

$$\begin{aligned} L_{MN} &= \partial_M L_N - \partial_N L_M - i\,[L_M, L_N], \\ R_{MN} &= \partial_M R_N - \partial_N R_M - i\,[R_M, R_N], \end{aligned} \tag{4}$$

with $L_M = L_M^a\,t^a$ and $R_M = R_M^a\,t^a$. Moreover, the non-abelian gauge fields and the scalar one interact through the covariant derivative $D_M X = \partial_M X - i L_M X + i X R_M$. Vector

(V) and axial vector (A) fields can be written in terms of right-hand gauge fields as $V = (L + R)/2$ and $A = (L - R)/2$. In the above definitions, N_f is the number of flavours, and here we take $N_f = 4$, which means all of the light, strange and charmed mesons are included in our model. The scalar field X can be expanded in exponential form as:

$$X = e^{i\pi^a t^a} X_0 e^{i\pi^a t^a}, \tag{5}$$

where the background part is denoted by X_0 and π are (pseudoscalar) fluctuations. For the classical solution, we turn off all fields except X_0 and solve the equation of motion. Finally, we arrive at:

$$2X_0(z) = \zeta M z + \frac{\Sigma}{\zeta} z^3, \tag{6}$$

where M denotes the quark-mass matrix and Σ is the quark condensates $\langle \bar{q}q \rangle$ one. Moreover, $\zeta = \sqrt{N_c}/2\pi$ is the normalization parameter [70]. With flavour symmetry, Eq.(5) can be written as $X = e^{2i\pi^a t^a} X_0$, which is used to predict masses and decay constants of ground-state and excited light and strange mesons in [71,72]. With $N_f = 4$, we take $M = \text{diag}(m_u, m_d, m_s, m_c)$ and $\Sigma = \text{diag}(\sigma_u, \sigma_d, \sigma_s, \sigma_c)$.

To evaluate the wave functions of the particles included in this study, the action Eq. (3) must be expanded up to second order in vector (V), axial vector (A) and pseudoscalar field (π) as:

$$\begin{aligned} S = \int d^5x \Bigg\{ & \sum_{a=1}^{15} \frac{-1}{4g_5^2 z} \eta^{MM'} \eta^{NN'} (\partial_M V_N^a - \partial_N V_M^a) \\ & \times (\partial_{M'} V_{N'a} - \partial_{N'} V_{M'a}) + \frac{M_V^{a\,2}}{2z^3} \eta^{MM'} V_{Ma} V_{M'}^a \\ & \times \frac{-1}{4g_5^2 z} \eta^{MM'} \eta^{NN'} (\partial_M A_N^a - \partial_N A_M^a) \\ & \times (\partial_{M'} A_{N'a} - \partial_{N'} A_{M'a}) \\ & + \frac{M_A^{a\,2}}{2z^3} \eta^{MM'} (\partial_M \pi^a - A_M^a)(\partial_{M'} \pi_b - A_{M'b}) \Bigg\}, \end{aligned} \tag{7}$$

where the mass combinations are defined as:

$$\begin{aligned} M_V^{a\,2} \delta^{ab} &= -2\,\text{Tr}\,([t^a, X_0][t^b, X_0]), \\ M_A^{a\,2} \delta^{ab} &= 2\,\text{Tr}\,(\{t^a, X_0\}\{t^b, X_0\}). \end{aligned} \tag{8}$$

The values of $M_V^{a\,2}$ and $M_A^{a\,2}$ for $(a = 1, \ldots, 15)$, calculated in [68], are collected in the Appendix. In the following subsection, we consider the axial sector and the vector one from action (7) to study the wave functions, decay constant and masses of physical particles.

2.1 Axial sector

The axial vector field (A_N) satisfies the equation of motion as:

$$\eta^{ML} \partial_M \left(\frac{1}{z} \left(\partial_L A_N^a - \partial_N A_L^a \right) \right) + \frac{\beta^a(z)}{z} A_N^a = 0, \tag{9}$$

where we have defined:

$$\beta^a(z) = \frac{g_5^2}{z^2} M_A^{a\,2}. \tag{10}$$

Now in Eq. (9), we write $A_N^a = (A_\mu^a, A_z^a)$ and make the decomposition $A_\mu^a = A_{\mu\perp}^a + A_{\mu\parallel}^a$. For the transverse part, which describes the axial vector states, $(A_{\mu\perp}^a)$, we can write:

$$\left(\partial_z \frac{1}{z} \partial_z + \frac{q^2 - \beta^a}{z} \right) A_{\mu\perp}^a(q, z) = 0, \tag{11}$$

in a gauge where $A_z^a = 0$. Here q is the Fourier variable conjugate to the 4-dimensional coordinates, x. We shall write the transverse part of the axial vector field in terms of its boundary values at UV $(A_{\mu\perp}^{0a})$ multiplying bulk-to-boundary propagator $(\mathcal{A}^a)$, $A_{\mu\perp}^a(q, z) = A_{\mu\perp}^{0a}(q) \mathcal{A}^a(q^2, z)$. $\mathcal{A}^a(q^2, z)$ satisfies the same equation as $A_{\mu\perp}^a(q, z)$ with the boundary conditions $\mathcal{A}^a(q^2, \varepsilon) = 1$ and $\partial_z \mathcal{A}^a(q^2, z_0) = 0$. The longitudinal part of the axial vector field, defined as $A_{\mu\parallel}^a = \partial_\mu \phi^a$ and π^a, describe the pseudoscalar fields and satisfy the following equations:

$$-q^2 \partial_z \phi^a(q^2, z) + \beta^a(z) \partial_z \pi^a(q^2, z) = 0\,, \tag{12}$$

$$\partial_z \left(\frac{1}{z} \partial_z \phi^a(q^2, z) \right) - \frac{\beta^a(z)}{z} \times \left(\phi^a(q^2, z) - \pi^a(q^2, z) \right) = 0\,, \tag{13}$$

with the boundary conditions, $\phi^a(q^2, \varepsilon) = 0$, $\pi^a(q^2, \varepsilon) = -1$, and $\partial_z \phi^a(q^2, z_0) = \partial_z \pi^a(q^2, z_0) = 0$. In general, the form of differential equations Eqs. (11, 12, 13), $\mathcal{A}^a(q^2, z)$, $\phi^a(q^2, z)$ and $\pi^a(q^2, z)$ can be solved numerically.

Using Green's function formalism to solve Eqs. (11, 12, 13), the bulk-to-boundary propagator $\mathcal{A}^a$, π^a and ϕ^a can be written as a sum over axial vector and pseudoscalar mesons poles as:

$$\begin{aligned} \mathcal{A}^a(q^2, z) &= \sum_n \frac{-g_5 f_{A^n}^a \psi_{A^n}^a(z)}{q^2 - m_{A^n}^{a2}}\,, \\ \phi^a(q^2, z) &= \sum_n \frac{-g_5 m_{pn}^{a2} f_{pn}^a \phi_n^a(z)}{q^2 - m_{pn}^{a2}}\,, \\ \pi^a(q^2, z) &= \sum_n \frac{-g_5 m_{pn}^{a2} f_{pn}^a \pi_n^a(z)}{q^2 - m_{pn}^{a2}}\,, \end{aligned} \tag{14}$$

where f_{A^n} and (f_{P^n}) are decay constants of the n^{th} axial vector meson and the pseudoscalar one and for the n^{th} axial vector meson's wave function are $\psi_{A^n}(\epsilon) = 0$ and

$\partial_z \psi_{A^n}(z_0) = 0$ are the boundary conditions. Moreover, for the pseudoscalar meson's wave functions, the boundary conditions are: $\phi_n^a(\varepsilon) = \pi_n^a(\varepsilon) = 0$ and $\partial_z \phi_n^a(z_0) = \partial_z \pi_n^a(z_0) = 0$ and the normalization condition for these wavefunctions is $\int (dz/z) g(z)^2 = 1$ for $g = \psi^a_{A^n}, \pi^a_n, \phi^a_n$. The decay constants of the n^{th} mode of the axial vector and the pseudoscalar states are related to their nth wave functions as [69]:

$$f^a_{A^n} = \left.\frac{\partial_z \psi^a_{A^n}}{g_5\, z}\right|_{z=\epsilon}, \tag{15}$$

$$f^a_{P^n} = -\left.\frac{\partial_z \phi^a_n}{g_5\, z}\right|_{z=\epsilon}. \tag{16}$$

With $N_f = 4$, the axial vector A and the pseudoscalar π involves the light, strange and charmed states can be written as follows:

$$A = A^a t^a = \frac{1}{\sqrt{2}} \begin{pmatrix} \frac{a_1^0+b_1^0}{\sqrt{2}} + \frac{f_1+f_1'}{\sqrt{6}} + \frac{\chi_{c1}}{\sqrt{12}} & a_1^+ + b_1^+ & K_{1A}^+ + K_{1B}^+ & \bar{D}_1^0 \\ a_1^- + b_1^- & -\frac{a_1^0+b_1^0}{\sqrt{2}} + \frac{f_1+f_1'}{\sqrt{6}} + \frac{\chi_{c1}}{\sqrt{12}} & K_{1A}^0 + K_{1B}^0 & D_1^- \\ K_{1A}^- + K_{1B}^- & \bar{K}_{1A}^0 + \bar{K}_{1B}^0 & -\sqrt{\frac{2}{3}}(f_1 + f_1') + \frac{\chi_{c1}}{\sqrt{12}} & D_{s1}^- \\ D_1^0 & D_1^+ & D_{s1}^+ & -\frac{3}{\sqrt{12}}\chi_{c1} \end{pmatrix},$$

$$\pi = \pi^a t^a = \frac{1}{\sqrt{2}} \begin{pmatrix} \frac{\pi^0}{\sqrt{2}} + \frac{\eta}{\sqrt{6}} + \frac{\eta_c}{\sqrt{12}} & \pi^+ & K^+ & \bar{D}^0 \\ \pi^- & -\frac{\pi^0}{\sqrt{2}} + \frac{\eta}{\sqrt{6}} + \frac{\eta_c}{\sqrt{12}} & K^0 & D^- \\ K^- & \bar{K}^0 & -\sqrt{\frac{2}{3}}\eta + \frac{\eta_c}{\sqrt{12}} & D_s^- \\ D^0 & D^+ & D_s^+ & -\frac{3}{\sqrt{12}}\eta_c \end{pmatrix}.$$

The physical states $K_1(1270)$ and $K_1(1400)$ mesons are related to K_{1A} and K_{1B} states in terms of a mixing angle θ_K as the following terms:

$$K_1(1270) = \sin\theta_K\, K_{1A} + \cos\theta_K\, K_{1B}, \tag{17}$$

$$K_1(1400) = \cos\theta_K\, K_{1A} - \sin\theta_K, K_{1B}. \tag{18}$$

Various approaches have been utilized to estimate the mixing angle θ_K by the experimental data. The result $35^\circ < |\theta_K| < 55^\circ$ was found in Ref. [73], and two possible solutions with $|\theta_K| \approx 33^\circ$ and 57° were reported in Ref. [74]. Moreover, the value $\theta_K = -(34 \pm 13)^\circ$ is obtained via analyzing $B \to K_1(12070)\gamma$ and $\tau \to K_1(12070)\,\nu_\tau$ data in [75].

2.2 Vector sector

The equation of motion for the vector field (V_N) is similar to Eq. (9) by replacing the $V_N \to A_N$ and $\beta^a \to \alpha^a(z) = (g_5^2/z^2)\, M_V^{a\,2}$. Writing $V_N^a = (V_\mu^a, V_z^a)$ and $V_\mu^a = V_{\mu\perp}^a + V_{\mu\|}^a$ and applying $\partial^\mu V_{\mu\perp}^a(x,z) = 0$, for the transverse part of the vector field, which represents the vector meson states, the following result is obtained:

$$\left(\partial_z \frac{1}{z}\partial_z + \frac{q^2 - \alpha^a}{z}\right) V_{\mu\perp}^a(q,z) = 0. \tag{19}$$

Now, we consider $V_{\mu\perp}^a(q,z) = V_{\mu\perp}^{0a}(q)\mathcal{V}^a(q^2,z)$, where $\mathcal{V}^a(q^2,z)$ satisfies the same equation as (19) with the boundary conditions $\mathcal{V}^a(q^2,\varepsilon) = 1$ and $\partial_z \mathcal{V}^a(q^2,z_0) = 0$. The longitudinal parts of the vector field, defined as $V_{\mu\|}^a = \partial_\mu \xi^a$ and $V_z^a = -\partial_z \tilde{\pi}^a$, describe the scalar states and are coupled as follows:

$$-q^2 \partial_z \tilde{\phi}^a(q^2,z) + \alpha^a \partial_z \tilde{\pi}^a(q^2,z) = 0\,, \tag{20}$$

$$\partial_z\left(\frac{1}{z}\partial_z \tilde{\phi}^a(q^2,z)\right) - \frac{\alpha^a}{z}\left(\tilde{\phi}^a(q^2,z) - \tilde{\pi}^a(q^2,z)\right) = 0, \tag{21}$$

where $\xi^a = \tilde{\phi}^a - \tilde{\pi}^a$. The boundary conditions for ϕ^a and π^a are $\tilde{\phi}^a(q,\varepsilon) = 0$, $\tilde{\pi}^a(q,\varepsilon) = -1$ and $\partial_z \tilde{\phi}^a(q^2,z_0) = \partial_z \tilde{\pi}^a(q^2,z_0) = 0$.

For $\mathcal{V}^a$, $\tilde{\phi}^a$ and $\tilde{\pi}^a$, the Green functions are:

$$\mathcal{V}^a(q^2,z) = \sum_n \frac{-g_5 f^a_{V^n} \psi^a_{V^n}(z)}{q^2 - m^{a2}_{V^n}},$$

$$\tilde{\phi}^a(q^2,z) = \sum_n \frac{-g_5 m^{a2}_{s^n} f^a_{s^n} \tilde{\phi}^a_n(z)}{q^2 - m^{a2}_{s^n}},$$

$$\tilde{\pi}^a(q^2,z) = \sum_n \frac{-g_5 m^{a2}_{s^n} f^a_{s^n} \tilde{\pi}^a_n(z)}{q^2 - m^{a2}_{s^n}}. \tag{22}$$

The decay constants of the n^{th} mode of the vector meson and the scalar one have been obtained as [69]:

$$f^a_{V^n} = \left.\frac{\partial_z \psi^a_{V^n}}{g_5\, z}\right|_{z=\epsilon},$$

$$f^a_{s^n} = -\left.\frac{\partial_z \tilde{\phi}^a_n}{g_5\, z}\right|_{z=\epsilon}. \tag{23}$$

Finally, the SU(4) vector V and pseudoscalar $\tilde{\pi}$ meson matrices in terms of the charged states are introduced as follows:

$$V = V^a t^a = \frac{1}{\sqrt{2}} \begin{pmatrix} \frac{\rho^0}{\sqrt{2}} + \frac{\omega'}{\sqrt{6}} + \frac{\psi}{\sqrt{12}} & \rho^+ & K^{*+} & \bar{D}^{*0} \\ \rho^- & -\frac{\rho^0}{\sqrt{2}} + \frac{\omega'}{\sqrt{6}} + \frac{\psi}{\sqrt{12}} & K^{*0} & D^{*-} \\ K^{*-} & \bar{K}^{*0} & -\sqrt{\frac{2}{3}}\omega' + \frac{\psi}{\sqrt{12}} & D_s^{*-} \\ D^{*0} & D^{*+} & D_s^{*+} & -\frac{3}{\sqrt{12}}\psi \end{pmatrix},$$

$$S = \tilde{\pi}^a t^a = \frac{1}{\sqrt{2}} \begin{pmatrix} \frac{a_0^0}{\sqrt{2}} + \frac{\sigma}{\sqrt{6}} + \frac{\chi_{c0}}{\sqrt{12}} & a_0^+ & K_0^+ & \bar{D}_0 \\ a_0^- & -\frac{a_0^0}{\sqrt{2}} + \frac{\sigma}{\sqrt{6}} + \frac{\chi_{c0}}{\sqrt{12}} & K_0 & D_0^- \\ K_0^- & \bar{K}_0 & -\sqrt{\frac{2}{3}}\sigma + \frac{\chi_{c0}}{\sqrt{12}} & D_{0s}^- \\ D_0 & D_0^+ & D_{0s}^+ & -\frac{3}{\sqrt{12}}\chi_{c0} \end{pmatrix},$$

3 $D \to (V, A, S)\,\ell\,\nu_\ell$ form factors

In this section, the form factors of $D \to (V, A, S)\ell\,\nu_\ell$ are derived in Hard-Wall AdS/QCD model. At the quark level, this process is induced by the semileptonic decay of charm quark $c \to q\,\ell\,\nu_\ell$ with $q = d, s$. Considering $q = d$, the decays $D^0 \to \rho^-(b_1^-, a_1^-, a_0^-)\,\ell\,\nu_\ell$ and $D_s^+ \to K_0(K_{1A}^0, K_{1B}^0)\,\ell\,\nu_\ell$ have been studied, and for $q = s$, the $D^0 \to K^{*-}(K_{1A}^-, K_{1B}^-, K_0^-)\,\ell\,\nu_\ell$ and $D^- \to \bar{K}_0(\bar{K}_{1A}^0, \bar{K}_{1B}^0)\,\ell\,\nu_\ell$ processes are considered.

In the standard model of particle physics, the semileptonic decays $D \to M\,\ell\,\nu_\ell$ with $M = (V, A, S)$ are described by the following effective Hamiltonian:

$$\mathcal{H}_{eff} = \alpha(M)\,\frac{G_f}{\sqrt{2}} V_{cq}\,\left(\bar{q}\,\gamma_\mu(1-\gamma_5)\,c\right)\left(\bar{\ell}\,\gamma^\mu(1-\gamma_5)\,\nu_\ell\right), \tag{24}$$

where we take $\alpha(V, S) = 1$ and for $M = A$, $\alpha(M) = -1$. Moreover, G_F is the Fermi constant, and V_{cq} is the CKM matrix elements. The decay amplitude for these decays is obtained by inserting Eq. (24) between the initial meson D and final state M as:

$$\mathcal{M} = \alpha(M)\,\frac{G_f}{\sqrt{2}} V_{cq} \times \langle M(p_2)|\bar{q}\,\gamma_\mu(1-\gamma_5)\,c|D(p)\rangle\,\left(\bar{\ell}\,\gamma^\mu(1-\gamma_5)\,\nu_\ell\right), \tag{25}$$

where p_1 and p_2 are the momentum of D and M states, respectively. To evaluate the decay amplitude ($\mathcal{M}$), we need to calculate the matrix elements $\langle M(p_2)|\bar{q}\,\gamma_\mu\,c|D(p)\rangle$ and $\langle M(p_2)|\bar{q}\,\gamma_\mu\,\gamma_5 c|D(p)\rangle$. These matrix elements can be parameterized in terms of the form factors. For $M = V$, these matrix elements are defined as:

$$\langle V(p_2,\varepsilon_V)|\bar{q}\,\gamma_\mu\,c|D(p_1)\rangle = \varepsilon^*_{V\mu}\,m_D\,m_V\,\frac{2\,V(q^2)}{(m_D+m_V)}, \tag{26}$$

$$\langle V(p_2,\varepsilon_V)|\bar{q}\,\gamma_\mu\,\gamma_5\,c|D(p_1)\rangle = i\,\varepsilon^*_{V\mu}\,(m_D+m_V)\,A_1(q^2) - i\,(p_1+p_2)_\mu\,(\varepsilon^*_V.q)\,\frac{A_2(q^2)}{(m_D+m_V)} - i\,q_\mu\,(\varepsilon^*_V.q)\,\frac{2\,m_V}{q^2}\,[A_3(q^2)-A_0(q^2)], \tag{27}$$

where ε_V is the polarization vector of V meson and $q = p_1 - p_2$ is the transport momentum. In Eqs. (26) and (27), $V(q^2)$ and $A_i(q^2)$ with $(i = 0, \ldots, 3)$ are the transition form factors of the $D \to V\,\ell\,\nu_\ell$ decay. Form factor $A_3(q^2)$ can be written as a linear combination of $A_1(q^2)$ and $A_2(q^2)$ as:

$$A_3(q^2) = \frac{(m_D+m_V)}{2\,m_V}\,A_1(q^2) - \frac{(m_D-m_V)}{2\,m_V}\,A_2(q^2), \tag{28}$$

with the condition $A_0(0) = A_3(0)$.
For $M = A$, the transition form factors $A(q^2)$ and $V_i(q^2)$ with $(i = 0, \ldots, 3)$ are defined as:

$$\langle A(p_2,\varepsilon_A)|\bar{q}\,\gamma_\mu\,\gamma_5\,c|D(p_1)\rangle = \varepsilon^*_{A\mu}\,m_D\,m_A\,\frac{2i\,A(q^2)}{(m_D-m_A)}, \tag{29}$$

$$\langle A(p_2,\varepsilon_A)|\bar{q}\,\gamma_\mu\,c|D(p_1)\rangle = \varepsilon^*_{A\mu}\,(m_D-m_A)\,V_1(q^2) - (p_1+p_2)_\mu(\varepsilon^*_A.q)\frac{V_2(q^2)}{(m_D-m_A)} - q_\mu\,(\varepsilon^*_A.q)\,\frac{2\,m_A}{q^2}[V_3(q^2)-V_0(q^2)], \tag{30}$$

where ε_A is the polarization vector of the axial-vector meson A, $V_0(0) = V_3(0)$ and

$$V_3(q^2) = \frac{(m_D - m_A)}{2\,m_A}\,V_1(q^2) - \frac{(m_D + m_A)}{2\,m_A}\,V_2(q^2). \quad (31)$$

And finally, the form factors of $D \to S\,\ell\,\nu_\ell$ are defined as:

$$\langle\ S(p_2)|\bar{q}\,\gamma_\mu\,\gamma_5\,c|D(p_1)\rangle = (p_1 + p_2)_\mu\,f_+(q^2) + q_\mu\frac{m_D^2 - m_S^2}{q^2}\,[f_-(q^2) - f_+(q^2)], \quad (32)$$

with $f_-(0) = f_+(0)$.

To evaluate the form factors of $D \to (V, A, S)\,\ell\,\nu_\ell$ in Hard-Wall AdS/QCD, we start with the correlation function, including the currents of 3 involving particles. These 3-point functions can be obtained by functionally differentiating the 5-D action with respect to their sources, which are taken to be boundary values of the 5-D fields that have the correct quantum numbers as [36,37,76,77]:

$$\langle 0|\mathcal{T}\ \{J^{\mu a}_{V\perp}(x)J^{\nu b}_{V\perp}(y)J^{\alpha c}_{A\parallel}(w)\}|0\rangle = -\frac{\delta^3\mathrm{S(VVP)}}{\delta V^{0a}_{\perp\mu}(x)\,\delta V^{0b}_{\perp\nu}(y)\,\delta A^{0c}_{\parallel\alpha}(w)}, \quad (33)$$

$$\langle 0|\mathcal{T}\ \{J^{\mu a}_{V\perp}(x)J^{\nu b}_{A\perp}(y)J^{\alpha c}_{A\parallel}(w)\}|0\rangle = -\frac{\delta^3\mathrm{S(VAP)}}{\delta V^{0a}_{\perp\mu}(x)\,\delta A^{0b}_{\perp\nu}(y)\,\delta A^{0c}_{\parallel\alpha}(w)}, \quad (34)$$

$$\langle 0|\mathcal{T}\ \{J^{\mu a}_{A\perp}(x)J^{\nu b}_{A\perp}(y)J^{\alpha c}_{A\parallel}(w)\}|0\rangle = -\frac{\delta^3\mathrm{S(AAP)}}{\delta A^{0a}_{\perp\mu}(x)\,\delta A^{0b}_{\perp\nu}(y)\,\delta A^{0c}_{\parallel\alpha}(w)}, \quad (35)$$

$$\langle 0|\mathcal{T}\ \{J^{\mu a}_{A\perp}(x)J^{\nu b}_{V\perp}(y)J^{\alpha c}_{A\parallel}(w)\}|0\rangle = -\frac{\delta^3\mathrm{S(AVP)}}{\delta A^{0a}_{\perp\mu}(x)\,\delta V^{0b}_{\perp\nu}(y)\,\delta A^{0c}_{\parallel\alpha}(w)}, \quad (36)$$

$$\langle 0|\mathcal{T}\ \{J^{\alpha a}_{V\parallel}(x)J^{\mu b}_{A\perp}(y)J^{\beta c}_{A\parallel}(w)\}|0\rangle = -\frac{\delta^3\mathrm{S(SAP)}}{\delta V^{0a}_{\parallel\alpha}(x)\,\delta A^{0b}_{\perp\mu}(y)\,\delta A^{0c}_{\parallel\beta}(w)}, \quad (37)$$

where $\mathrm{S(M_1\,M_2\,M_3)}$ is the relevant parts of the 5-D action, including $(M_1\ M_2\ M_3)$ states. Here, Eqs. (33, 34) are used to evaluate the form factors of $D \to V\,\ell\,\nu_\ell$ decays while Eqs. (35, 36) are written for the correlation functions of $D \to A\,\ell\,\nu_\ell$ process, and Eq. (37) is noted as the first step in evaluating the form factors of $D \to S\,\ell\,\nu_\ell$ decay in Hard-Wall AdS/QCD.

To evaluate the form factors, we insert two complete sets of intermediate states with the same quantum numbers as the initial and final meson currents, and use the following definitions:

$$\langle 0|J^{\sigma a}_{V\perp}|V^{a'}(p,\varepsilon_V)\rangle = f_V\,\varepsilon_V^\sigma\,\delta^{aa'}, \quad (38)$$

$$\langle 0|J^{\alpha d}_{A\parallel}|\phi^{d'}(p)\rangle = i f_P^d\,p^\alpha\delta^{dd'}, \quad (39)$$

$$\langle 0|J^{\sigma a}_{A\perp}|A^{a'}(p,\varepsilon)\rangle = f_A\,\varepsilon_A^\sigma\,\delta^{aa'}, \quad (40)$$

$$\langle 0|J^{\alpha d}_{V\parallel}|\tilde{\phi}^{d'}(p)\rangle = i f_S^d\,p^\alpha\delta^{dd'}, \quad (41)$$

where f_V, f_P, f_A and f_S are the decay constants of the vector, pseudoscalar, axial vector and scalar mesons, respectively. In this step, the following results can be obtained:

$$\langle V^a(p_2,\varepsilon_V)|J^{vb}_{V\perp}(0)|D^c(p_1)\rangle = i\,\Lambda[(V,p_2);(D,p_1)]\,\Omega_\alpha(p_1)\varepsilon^*_{V\mu}\,\hat{\mathcal{I}} \times\left(\frac{\delta^3\mathrm{S(VVP)}}{\delta V^{0a}_{\perp\mu}(x)\,\delta V^{0b}_{\perp\nu}(0)\,\delta A^{0c}_{\parallel\alpha}(w)}\right), \quad (42)$$

$$\langle V^a(p_2,\varepsilon_V)|J^{vb}_{A\perp}(0)|D^c(p)\rangle = i\,\Lambda[(V,p_2);(D,p_1)]\,\Omega_\alpha(p_1)\,\varepsilon^*_{V\mu}\,\hat{\mathcal{I}} \times\left(\frac{\delta^3\mathrm{S(VAP)}}{\delta V^{0a}_{\perp\mu}(x)\,\delta A^{0b}_{\perp\nu}(0)\,\delta A^{0c}_{\parallel\alpha}(w)}\right), \quad (43)$$

$$\langle A^a(p_2,\varepsilon_A)|J^{vb}_{A\perp}(0)|D^c(p_1)\rangle = i\,\Lambda[(A,p_2);(D,p_1)]\,\Omega_\alpha(p_1)\varepsilon^*_{A\mu}\,\hat{\mathcal{I}} \times\left(\frac{\delta^3\mathrm{S(AAP)}}{\delta A^{0a}_{\perp\mu}(x)\,\delta A^{0b}_{\perp\nu}(0)\,\delta A^{0c}_{\parallel\alpha}(w)}\right), \quad (44)$$

$$\langle A^a(p_2,\varepsilon_A)|J^{vb}_{V\perp}(0)|D^c(p)\rangle = i\,\Lambda[(A,p_2);(D,p_1)]\,\Omega_\alpha(p_1)\,\varepsilon^*_{A\mu}\,\hat{\mathcal{I}} \times\left(\frac{\delta^3\mathrm{S(AVP)}}{\delta A^{0a}_{\perp\mu}(x)\,\delta V^{0b}_{\perp\nu}(0)\,\delta A^{0c}_{\parallel\alpha}(w)}\right), \quad (45)$$

$$\langle S^a(p_2)|J^{\mu b}_{A\perp}(0)|D^c(p)\rangle = i\,\Lambda[(S,p_2);(D,p_1)]\,\Omega_\alpha(p_1)\,\Omega_\beta(p_2)\,\hat{\mathcal{I}} \times\left(\frac{\delta^3\mathrm{S(SAP)}}{\delta V^{0a}_{\parallel\alpha}(x)\,\delta A^{0b}_{\perp\mu}(0)\,\delta A^{0c}_{\parallel\beta}(w)}\right), \quad (46)$$

where

$$\hat{\mathcal{I}} = \int d^4x\,d^4w\,e^{ip'x - ipw}, \quad \Omega_\alpha(p_k) = \frac{p_{k\alpha}}{p_k^2}, \quad \Lambda[(\mathcal{O}_2,p_2);(\mathcal{O}_1,p_1)] = \frac{(p_1^2 - m^2_{\mathcal{O}_1})}{f_{\mathcal{O}_1}}\,\frac{(p_2^2 - m^2_{\mathcal{O}_2})}{f_{\mathcal{O}_2}}, \quad (47)$$

are defined in our notations. Moreover, $f_{\mathcal{O}_i}$ is the decay constant of the i^{th} meson, and the limit $(p_1^2, p_2^2) \to (m^2_{\mathcal{O}_1}, m^2_{\mathcal{O}_2})$ is taken in the final result. Now, we need the relevant actions presented in Eqs. (42, 43, 44, 45, 46). For example, two vector mesons and one pseudoscalar state are separated from the total action for S(VVP). One vector meson, one axial vector and one pseudoscalar meson are also considered for S(VAP). These relevant actions are calculated in our recent paper as [68]:

$$\mathrm{S(VVP)} = \int d^5x\left(\frac{k^{abc}}{z^3}\,[V_\mu^a\,V^{\mu b}\,\pi^c + V_z^a\,V^{zb}\,\pi^c]\right), \quad (48)$$

$$\mathrm{S(VAP)} = \int d^5x \Big(\frac{f^{abc}}{2\, g_5^2\, z} \, [\partial^\mu \phi^b \, V_{\mu\nu} \, A^{\nu c}] + \frac{h^{abc}}{z^3} \, [V^{a\mu} \, A^b_\mu \pi^c] + \frac{g^{abc}}{z^3} \, [A^a_\mu \, V^{b\mu} \, \pi^c] \Big), \tag{49}$$

$$\mathrm{S(AAP)} = \int d^5x \Big(\frac{l^{abc}}{z^3} \, [A^a_\mu \, A^{\mu b} \, \pi^c] \Big), \tag{50}$$

$$\mathrm{S(SAP)} = \int d^5x \Big(\frac{h^{abc}}{z^3} \, [\partial^\mu (\tilde{\pi}^a - \tilde{\phi}^a) \, A^b_\mu \pi^c] + \frac{g^{abc}}{z^3} \, [A^a_\mu \, \partial^\mu (\tilde{\pi}^b - \tilde{\phi}^b) \, \pi^c] \Big), \tag{51}$$

where f^{abc} is the $SU(4)$ structure constant and the terms containing this factor are generated from the gauge part of the main action. The following definitions are also used in Eqs. (48–51):

$$k^{abc} = -2i \, \mathrm{Tr} \left(\left[t^a, X_0 \right] \left[t^b, \left\{ t^c, X_0 \right\} \right] \right), \tag{52}$$

$$h^{abc} = -2i \, \mathrm{Tr} \left(\left[t^a, X_0 \right] \left\{ t^b, \left\{ t^c, X_0 \right\} \right\} \right), \tag{53}$$

$$g^{abc} = -2i \, \mathrm{Tr} \left(\left\{ t^a, X_0 \right\} \left[t^b, \left\{ t^c, X_0 \right\} \right] \right), \tag{54}$$

$$l^{abc} = -2\, i \, \mathrm{Tr} \left(\left\{ t^a, X_0 \right\} \left\{ t^b, \left\{ t^c, X_0 \right\} \right\} \right). \tag{55}$$

The values of f^{abc} are taken from [78]. Moreover, the other values of k^{abc}, h^{abc} and g^{abc}, which are used in the numerical part, are collected in the Appendix. Using the Fourier transforms as [58,79]:

$$\begin{aligned} \phi^a(p,z) &= \phi^a(p^2,z) \frac{ip^\alpha}{p^2} A^{0a}_{\parallel\alpha}(p)\,, \\ \pi^a(p,z) &= \pi^a(p^2,z) \frac{ip^\alpha}{p^2} A^{0a}_{\parallel\alpha}(p)\,, \end{aligned} \tag{56}$$

$$\begin{aligned} A^a_{\perp\mu}(q,z) &= \mathcal{A}^a(q^2,z) \; A^{0a}_{\perp\mu}(q), \\ V^b_{\perp\mu}(q,z) &= \mathcal{V}^b(q^2,z) \; V^{0b}_{\perp\mu}(q)\,, \end{aligned} \tag{57}$$

$$\begin{aligned} V^b_z(q,z) &= -\partial_z \tilde{\pi}^b(q^2,z) \; \frac{iq^\alpha}{q^2} V^{0b}_{\parallel\alpha}(q)\,, \\ \partial^\mu &\to -i \; (\text{relevant momentum})^\mu \;, \end{aligned} \tag{58}$$

the form factors of $D \to V\, \ell\, \nu_\ell$ can be obtained as:

$$V(q^2) = \frac{(m_D + m_V)\, g_5^2}{2\, m_D\, m_V} \times \int_0^{z_m} dz \, \frac{k^{abc}}{z^3} \, \psi^a_V(z) \, \mathcal{V}^b(q^2,z) \, \pi^c(z), \tag{59}$$

$$\begin{aligned} A_1(q^2) = {} & \frac{g_5^2 \, (m_D^2 + m_V^2 - q^2)}{2\,(m_D + m_V)} \times \int_0^{z_m} dz \, \frac{f^{abc}}{4\,z} \, \phi^a(z) \, \psi^b_V(z) \, \mathcal{A}^c(q^2,z) \\ & + \frac{g_5^2}{2\,(m_D + m_V)} \int_0^{z_m} dz \times \Big[\frac{h^{abc}}{z^3} \, \psi^a_V(z) \, \mathcal{A}^b(q^2,z) \, \pi^c + \frac{g^{abc}}{z^3} \, \mathcal{A}^a(q^2,z) \, \psi^b_V(z) \pi^c \Big], \end{aligned} \tag{60}$$

$$A_2(q^2) = g_5^2 \, (m_D + m_V) \times \int_0^{z_m} dz \, \frac{f^{abc}}{4\,z} \, \phi^a(z) \, \psi^b_V(z) \, \mathcal{A}^c(q^2,z), \tag{61}$$

$$\begin{aligned} A_0(q^2) = {} & \frac{g_5^2 \, (3\, m_V^2 - q^2 - m_D^2)}{4\, m_V} \times \int_0^{z_m} dz \, \frac{f^{abc}}{4\,z} \, \phi^a(z) \, \psi^b_V(z) \, \mathcal{A}^c(q^2,z) \\ & + \frac{g_5^2}{4\, m_V} \int_0^{z_m} dz \Big[\frac{h^{abc}}{z^3} \, \psi^a_V(z) \, \mathcal{A}^b(q^2,z) \, \pi^c + \frac{g^{abc}}{z^3} \, \mathcal{A}^a(q^2,z) \, \psi^b_V(z) \pi^c \Big], \end{aligned} \tag{62}$$

and for $D \to A\, \ell\, \nu_\ell$ we have:

$$A(q^2) = \frac{(m_D - m_A)\, g_5^2}{2\, m_D\, m_A} \int_0^{z_m} dz \times \frac{l^{abc}}{z^3} \, \psi^a_V(z) \, \mathcal{A}^b(q^2,z) \, \pi^c(z), \tag{63}$$

$$\begin{aligned} V_1(q^2) = {} & \frac{g_5^2 \, (m_D^2 + m_A^2 - q^2)}{2\,(m_D - m_A)} \int_0^{z_m} dz \times \frac{f^{abc}}{4\,z} \, \phi^a(z) \, \mathcal{V}^b(q^2,z) \, \psi^c_A(z) \\ & + \frac{g_5^2}{2\,(m_D - m_A)} \int_0^{z_m} dz \times \Big[\frac{h^{abc}}{z^3} \, \psi^a_A(z) \, \mathcal{V}^b(q^2,z) \, \pi^c + \frac{g^{abc}}{z^3} \, \mathcal{V}^a(q^2,z) \, \psi^b_A(z) \pi^c \Big], \end{aligned} \tag{64}$$

$$V_2(q^2) = g_5^2 \, (m_D - m_A) \int_0^{z_m} dz \times \frac{f^{abc}}{4\,z} \, \phi^a(z) \, \psi^b_A(z) \, \mathcal{V}^c(q^2,z), \tag{65}$$

$$\begin{aligned} V_0(q^2) = {} & \frac{g_5^2 \, (3\, m_A^2 - q^2 - m_D^2)}{4\, m_A} \times \int_0^{z_m} dz \, \frac{f^{abc}}{4\,z} \, \phi^a(z) \, \psi^b_V(z) \, \mathcal{A}^c(q^2,z) \\ & + \frac{g_5^2}{4\, m_A} \int_0^{z_m} dz \Big[\frac{h^{abc}}{z^3} \, \psi^a_V(z) \, \mathcal{A}^b(q^2,z) \, \pi^c + \frac{g^{abc}}{z^3} \, \mathcal{A}^a(q^2,z) \, \psi^b_V(z) \pi^c \Big]. \end{aligned} \tag{66}$$

Finally, the form factors of $D \to S\,\ell\,\nu_\ell$ are resulted as:

$$
\begin{aligned}
f_+(q^2) = & \frac{g_5^2}{2}\int_0^{z_m} dz\,\frac{h^{abc}}{z^3}\,(\tilde{\pi}^a(z)-\tilde{\phi}^a(z)) \\
& \times \mathcal{A}^b(q^2,z)\,\pi^c(z) \\
& + \frac{g_5^2}{2}\int_0^{z_m} dz\,\frac{g^{abc}}{z^3}\,\mathcal{A}^a(q^2,z) \\
& \times (\tilde{\pi}^b(z)-\tilde{\phi}^b(z))\,\pi^c(z), \qquad (67)\\
f_-(q^2) = & \left(1-\frac{q^2}{m_D^2-m_S^2}\right)\frac{g_5^2}{2} \\
& \times \int_0^{z_m} dz\,\frac{h^{abc}}{z^3}\,(\tilde{\pi}^a(z) \\
& \times -\tilde{\phi}^a(z))\,\mathcal{A}^b(q^2,z)\,\pi^c(z) \\
& + \left(1-\frac{q^2}{m_D^2-m_S^2}\right)\frac{g_5^2}{2} \\
& \times \int_0^{z_m} dz\,\frac{g^{abc}}{z^3}\,\mathcal{A}^a(q^2,z) \\
& \times (\tilde{\pi}^b(z)-\tilde{\phi}^b(z))\,\pi^c(z),. \qquad (68)
\end{aligned}
$$

4 Numerical analysis

The numeric analysis for the masses, decay constants, and the wave functions of scalar mesons are presented in this section. Moreover, form factors and the branching ratios of D meson decays into vector, axial vector and scalar mesons are evaluated.

4.1 Wave functions and decay constants

First, we study the wave function of the mesons included in our model. To evaluate the wave function, we need to know the values of z_m, (m_u, m_d, m_s, m_c) and $(\sigma_u, \sigma_d, \sigma_s, \sigma_c)$. These values with their uncertain regions have already been evaluated using the experimental masses of ρ^0, ρ^-, a_1^-, π^0, π^-, K^-, K^{*-}, D^- and D^{*-} mesons in [68]. The best global fit for z_m is $z_m^{-1} = (323 \pm 1)$ MeV, and for the masses in MeV, the results are $m_u = (8.5 \pm 2.5)$, $m_d = (12.36 \pm 2.45)$, $m_s = (195.31 \pm 5.89)$ and $m_c = (1590.56 \pm 8.42)$. Moreover, for the quark condensates in MeV^3 the best global fit yields $\sigma_u = (173.65 \pm 2.21)^3$, $\sigma_d = (177.42 \pm 3.15)^3$, $\sigma_s = (226.20 \pm 3.72)^3$ and $\sigma_c = (310.35 \pm 5.65)^3$. The wave functions, masses, and decay constants of some vector, axial vector, and the pseudoscalar mesons are studied in [68], and here we focus on the scalar mesons. The results for the masses and the decay constants of the ground state scalar mesons a_0^-, K_0^-, K_0, D_0 and D_{0s}^- are listed in Table 1. In this table, the experimental values of masses as well as the QCD Sum Rule (QCDSR) predictions for the decay constants are also presented. The masses are taken from [80] and the decay constants are given in [81–83]. It should be noted that for neutral scalars a_0^0, σ and χ_{c0}, the differential equations take the form $\partial_z\tilde{\phi}^a(q^2,z) = 0$, and considering Eq. (23), for these states, the decay constant becomes zero. This result was predictable according to charge conjugation invariance or conservation of vector current.

It is possible to estimate the wave functions with the masses of physical states. The wave functions $\tilde{\phi}_S$ and $\tilde{\pi}_S$ for the ground states $S = (a_0^-, K_0^-, K_0, D_0, D_{0s}^-)$ are shown in Fig. 1 as functions of z/z_m. The dash, dotted, dash-dotted, dash-dot-dot and short-dash lines are utilized for $\tilde{\phi}^1$ and $\tilde{\pi}^1$ of a_0^-, K_0^-, K_0, D_0 and D_{0s}^-, respectively.

4.2 Form factors

To estimate the obtained form factors in Sect. 3, we need to know the masses of the initial states (D) and those of vector (V), axial vector (A), and scalar meson (S) as the final states. The used masses in numerical analysis are given in Table 2. The values for masses of ρ^-, K^{*-}, D^+ and a_1^- are taken from [80], while our model in [68] predicts the masses of D^0, D_s^+, K_{1A}^-. Moreover, for b_1^- and K_{1B}^- the predictions of the sum rule approach are inspired from [84].

At this point, we can estimate the form factors for each aforementioned semileptonic decay. The obtained results of the estimation for the form factors $[V, A_1, A_2, A_0]$, for $D \to V\,\ell\,\nu_\ell$ decays, $[A, V_1, V_2, V_0]$, for $D \to A\,\ell\,\nu_\ell$ decays, and f_+, for $D \to S\,\ell\,\nu_\ell$ transitions, at $q^2 = 0$, are presented in Table 3. Note that for $D \to S\,\ell\,\nu_\ell$ decays, we consider $f_+(0) = f_-(0)$. In the predictions for the form factors, the main uncertainty comes from the masses of the initial and final mesons, and the quark condensates σ_q.

The form factors of $D \to (V, A, S)\,\ell\,\nu_\ell$ decays are calculated with different theoretical frameworks. To compare the different results, we rescale them according to the form factor definitions in Eqs. (27, 30, 32). Table 4 shows the values of the rescaled form factors at $q^2 = 0$ for $D \to V\,\ell\,\nu_\ell$ decays, according to different theoretical approaches such as the LCSR [17], the 3PSR [27], the heavy quark effective field theory (HQETF) [85,86], the relativistic harmonic oscillator potential model (RHOPM) [87], the quark model [88,89], the light-front quark model (LFQM) [90], the heavy meson and chiral symmetries (HMχT) [91] and the LQCD [92]. The experimental measurements for the form factors of $D^0 \to \rho^-\,\ell\,\nu_\ell$, reported in CLEO [93], are also included in Table 4. In Table 5, a comparison is made between the estimation for the form factors of $D \to A\,\ell\,\nu_\ell$ decays obtained from this work and the 3PSR [34], the LCSR [18] and the LFQM [94] predictions. It is essential to note that for the $V(q^2)$ and $A(q^2)$ form factors, the presented parameterizations in Eqs. (26) and (29) are different from other methods, and we can not compare these form factors.

Table 1 Predictions for the masses and the decay constants of a_0^-, K_0^-, K_0, D_0 and D_{0s}^- scalar mesons. The experimental values for messes are reported in [80], while the QCDSR predictions for the decay constants are taken from [81–83]

Observable	m_S (MeV)		f_S (MeV)	
Scalar meson	This work	Experimental	This work	QCDSR
a_0^-	985.50 ± 4.52	980 ± 20	51.25 ± 8.96	47
K_0^-	1402 ± 5.20	1425 ± 50	46.86 ± 3.96	42
K_0	839 ± 2.16	845 ± 17	68.45 ± 3.82	65
D_0	2346 ± 9.80	2343 ± 10	211 ± 16.25	239 ± 73
D_{0s}^-	2326 ± 15.61	2317.8 ± 0.50	226 ± 17.54	283 ± 90

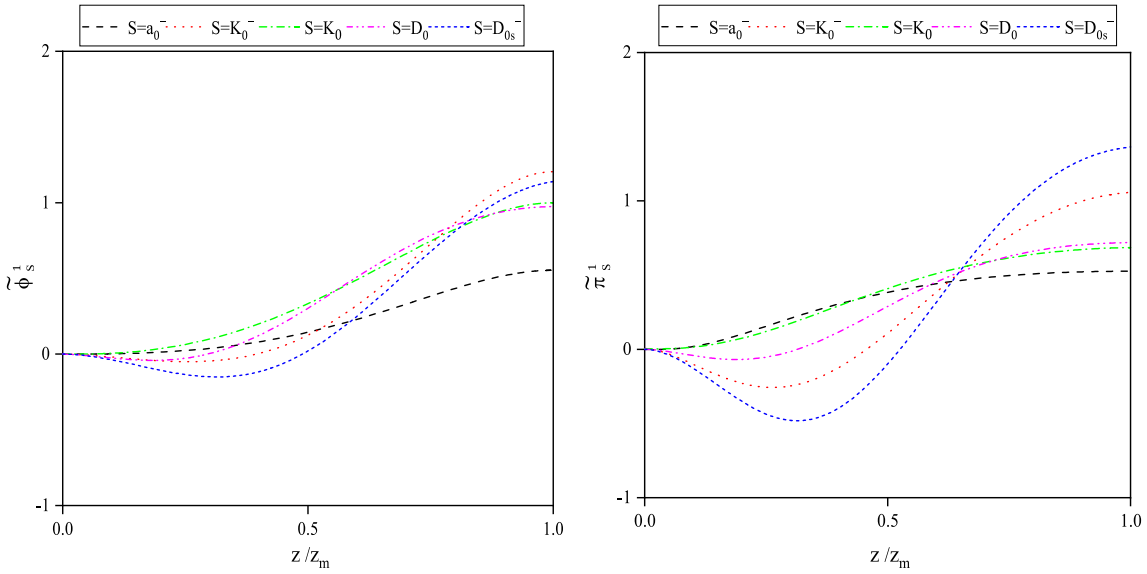

Fig. 1 The wave functions $\tilde{\phi}_S^1(z)$ and $\tilde{\pi}_S^1(z)$ for $S = (a_0^-, K_0^-, K_0, D_0, D_{0s}^-)$ as a function of z/z_m

Table 2 Masses for $D \to (V,\ A,\ S)\,\ell\,\nu_\ell$ decay's initial and final states as input parameters in presented numerical analysis. The experimental masses of ρ^-, K^{*-}, a_1^- and D^+ are taken from [80]. The values of D^0, D_s^+, K_{1A}^- are reported from Hard-Wall model [68]. $m_{b_1^-}$ and $m_{K_{1B}^-}$ are chosen from the results of sum rule method [84]

Meson	Mass (MeV)	Meson	Mass (MeV)	Meson	Mass (MeV)
ρ^-	775.49 ± 0.34	K^{*-}	891.66 ± 0.26	a_1^-	1230 ± 40
D^+	1869.65 ± 0.05	D^0	1861.50 ± 3.58	D_s^+	1972.63 ± 2.37
K_{1A}^-	1316.52 ± 7.50	b_1^-	1229.50 ± 3.20	K_{1B}^-	1340 ± 80

For the $D \to S\,\ell\,\nu_\ell$ category, only theoretical methods are used to study $D^0 \to a_0^-\,\ell\,\nu_\ell$. As can be noticed from Table 3, $f_+^{D^0\to a_0^-}(0) = (0.72 \pm 0.09)$ while, in CCQM [96] and LCSR [97], the results are predicted as: $f_+^{D^0\to a_0^-}(0) = (0.55 \pm 0.02)$ and $f_+^{D^0\to a_0^-}(0) = (1.75^{+0.26}_{-0.27})$, respectively.

To evaluate form factors as functions of q^2, it is important to note that q^2 varies in the interval $[m_\ell^2 \simeq 0\,,\ (m_D - m_M)^2]$ for the $D \to M\,\ell\,\nu_\ell$ decay, with $\ell = e, \mu$. From all the considered decays, the q^2 dependence of the form factors of $D^0 \to K^{*-}\,\ell\,\nu_\ell$, $D^0 \to a_1^-\,\ell\,\nu_\ell$, $D_s^+ \to K_{1A}^0\,\ell\,\nu_\ell$, $D_s^+ \to K_{1B}^0\,\ell\,\nu_\ell$, $D^0 \to a_0^-\,\ell\,\nu_\ell$ and $D^+ \to \bar{K}_0\,\ell\,\nu_\ell$ is selected and displayed in Fig. 2. In this figure, the form factors $V(A)$, $A_1(V_1)$, $A_2(V_2)$ and $A_0(V_0)$ are shown with the solid, dash, dash- dotted and dot lines, respectively. For decays to the scalar mesons, f_+ is shown with the solid line and, for f_- the dash line is utilized.

To obtain the form factors of $D \to K_1(1270)\,\ell\,\nu_\ell$ using Eqs. (17, 29, 30) the following relations are obtained:

$$A^{D\to K_1(1270)} = \Big(\frac{1-r_{K_1}}{1-r_{K_{1A}}}\Big)\Big(\frac{r_{K_{1A}}}{r_{K_1}}\Big)\,\sin\theta_K\,A^{D\to K_{1A}} + \Big(\frac{1-r_{K_1}}{1-r_{K_{1B}}}\Big)\Big(\frac{r_{K_{1B}}}{r_{K_1}}\Big)\,\cos\theta_K\,A^{D\to K_{1B}},$$

Table 3 The $D \to (V, A, S)\,\ell\,\nu_\ell$ form factors with their uncertainty regions, at zero momentum transfer in Hard-Wall AdS/QCD. Note that for scalar mesons as the final states, $f_+(0) = f_-(0)$

Form factor	Value at $q^2=0$	Form factor	Value at $q^2=0$	Form factor	Value at $q^2=0$	Form factor	Value at $q^2=0$
$V^{D^0\to\rho^-}$	0.29 ± 0.04	$V_0^{D^0\to a_1^-}$	-0.32 ± 0.06	$V_2^{D_s^+\to K_{1B}^0}$	0.23 ± 0.04	$V_1^{D^+\to \bar{K}_{1A}^0}$	0.54 ± 0.09
$A_1^{D^0\to\rho^-}$	0.54 ± 0.10	$A^{D^0\to b_1^-}$	0.12 ± 0.03	$V_0^{D_s^+\to K_{1B}^0}$	-0.17 ± 0.04	$V_2^{D^+\to \bar{K}_{1A}^0}$	0.37 ± 0.07
$A_2^{D^0\to\rho^-}$	0.40 ± 0.06	$V_1^{D^0\to b_1^-}$	0.57 ± 0.07	$A^{D^0\to K_{1A}^-}$	0.39 ± 0.04	$V_0^{D^+\to \bar{K}_{1A}^0}$	-0.33 ± 0.07
$A_0^{D^0\to\rho^-}$	0.63 ± 0.12	$V_2^{D^0\to b_1^-}$	0.32 ± 0.05	$V_1^{D^0\to K_{1A}^-}$	0.77 ± 0.12	$A^{D^+\to \bar{K}_{1B}^0}$	0.21 ± 0.03
$V^{D^0\to K^{*-}}$	0.34 ± 0.05	$V_0^{D^0\to b_1^-}$	-0.25 ± 0.05	$V_2^{D^0\to K_{1A}^-}$	0.60 ± 0.10	$V_1^{D^+\to \bar{K}_{1B}^0}$	0.48 ± 0.08
$A_1^{D^0\to K^{*-}}$	0.63 ± 0.12	$A^{D_s^+\to K_{1A}^0}$	0.23 ± 0.03	$V_0^{D^0\to K_{1A}^-}$	-0.22 ± 0.05	$V_2^{D^+\to \bar{K}_{1B}^0}$	0.27 ± 0.04
$A_2^{D^0\to K^{*-}}$	0.45 ± 0.07	$V_1^{D_s^+\to K_{1A}^0}$	0.51 ± 0.08	$A^{D^0\to K_{1B}^-}$	0.34 ± 0.05	$V_0^{D^+\to \bar{K}_{1B}^0}$	-0.18 ± 0.04
$A_0^{D^0\to K^{*-}}$	0.72 ± 0.13	$V_2^{D_s^+\to K_{1A}^0}$	0.28 ± 0.03	$V_1^{D^0\to K_{1B}^-}$	0.60 ± 0.11	$f_+^{D^0\to a_0^-}$	0.72 ± 0.09
$A^{D^0\to a_1^-}$	0.13 ± 0.03	$V_0^{D_s^+\to K_{1A}^0}$	-0.21 ± 0.05	$V_2^{D^0\to K_{1B}^-}$	0.42 ± 0.07	$f_+^{D_s^+\to K_0}$	0.95 ± 0.12
$V_1^{D^0\to a_1^-}$	0.59 ± 0.08	$A^{D_s^+\to K_{1B}^0}$	0.14 ± 0.03	$V_0^{D^0\to K_{1B}^-}$	-0.38 ± 0.07	$f_+^{D^0\to K_0^-}$	0.80 ± 0.10
$V_2^{D^0\to a_1^-}$	0.37 ± 0.04	$V_1^{D_s^+\to K_{1B}^0}$	0.46 ± 0.07	$A^{D^+\to \bar{K}_{1A}^0}$	0.31 ± 0.06	$f_+^{D^+\to \bar{K}_0}$	0.82 ± 0.10

Table 4 Transition form factors A_1, A_2 and A_0 of the $D \to V\,\ell\,\nu_\ell$ at $q^2 = 0$ in our model and other theoretical approaches

Model	$A_1(0)$	$A_2(0)$	$A_0(0)$	Model	$A_1(0)$	$A_2(0)$	$A_0(0)$
$D^0 \to \rho^-$							
This work	0.54 ± 0.10	0.40 ± 0.06	0.63 ± 0.12	RHOPM [87]	0.78	0.92	0.67
LCSR [17]	$0.580^{+0.065}_{-0.050}$	$0.468^{+0.052}_{-0.053}$		QM-I [88]	0.59	0.23	
CLEO (2013) [93]	$0.56^{+0.02}_{-0.03}$	0.47		QM-II [89]	0.59	0.49	
3PSR [27]	0.5	0.4		LFQM [90]	0.60	0.47	0.69
HQETF-I [85]	0.57 ± 0.08	0.52 ± 0.07		HMχT [91]	0.61	0.31	1.32
HQETF-II [86]	0.59 ± 0.03	$0.37^{+0.02}_{-0.03}$		LQCD [92]	$0.65^{+0.24}_{-0.23}$	$0.59^{+0.28}_{-0.25}$	$0.64^{+0.21}_{-0.21}$
$D^0 \to K^{*-}$							
This work	0.63 ± 0.12	0.45 ± 0.07	0.72 ± 0.13	RHOPM [87]	0.88	1.15	0.73
HQETF-I [85]	0.59 ± 0.10	0.55 ± 0.08		QM [89]	0.66	0.49	0.76
HQETF-II [86]	$0.57 \pm +0.02$	0.34 ± 0.03		LFQM-I [90]	0.72	0.60	0.78
HMχT [91]	1.12	0.31	1.32	LFQM-II [94]	0.65	0.57	0.69
3PSR [95]	0.50	0.60	0.40	Lattice QCD [92]	0.83 ± 0.28	$0.59^{+0.24}_{-0.23}$	

$$V_1^{D\to K_1(1270)} = \left(\frac{1-r_{K_{1A}}}{1-r_{K_1}}\right)\sin\theta_K\, V_1^{D\to K_{1A}} + \left(\frac{1-r_{K_{1B}}}{1-r_{K_1}}\right)\cos\theta_K\, V_1^{D\to K_{1B}}, \tag{70}$$

$$V_2^{D\to K_1(1270)} = \left(\frac{1-r_{K_1}}{1-r_{K_{1A}}}\right)\sin\theta_K\, V_2^{D\to K_{1A}} + \left(\frac{1-r_{K_1}}{1-r_{K_{1B}}}\right)\cos\theta_K\, V_2^{D\to K_{1B}}, \tag{71}$$

$$V_0^{D\to K_1(1270)} = \left(\frac{r_{K_{1A}}}{r_{K_1}}\right)\sin\theta_K\, V_0^{D\to K_{1A}} + \left(\frac{r_{K_{1B}}}{r_{K_1}}\right)\cos\theta_K\, V_0^{D\to K_{1B}}, \tag{72}$$

where on the right hand side of Eqs. (69–72), $K_1 = K_1(1270)$ and $r_M = m_D/m_M$. To evaluate the form factors of $D \to K_1(1400)\,\ell\,\nu_\ell$, the replacements of $\sin\theta_K \to \cos\theta_K$, $\cos\theta_K \to -\sin\theta_K$, and $K_1 \to K_1(1400)$ are required.

4.3 Branching ratios

To evaluate the branching ratio values for the $D \to (V, A, S)\,\ell\,\nu_\ell$ decays, the decay amplitude in Eq. (25), and definitions for the form factors given in Eqs. (26, 27, 29, 30, 32) are required. So, the differential decay widths are found

Table 5 The results for the transition form factors V_1, V_2 and V_0 of $D \to A\,\ell\,\nu_\ell$ decays at $q^2 = 0$, as well as predictions of 3PSR [33,34], LFQM [94] and LCSR [18]

$D^0 \to a_1^-$				$D^0 \to b_1^-$			
Model	$V_1(0)$	$V_2(0)$	$V_0(0)$	Model	$V_1(0)$	$V_2(0)$	$V_0(0)$
This work	0.59 ± 0.08	0.37 ± 0.04	-0.32 ± 0.06	This work	0.57 ± 0.07	0.32 ± 0.05	-0.32 ± 0.07
3PSR [34]	0.37	-0.03	0.15	LCSR [18]	-0.22	0.21	-0.32
LFQM [94]	1.54	0.06	0.31	LFQM [94]	1.37	-0.10	0.49
LCSR [18]	0.37 ± 0.11	-0.03 ± 0.02	0.15 ± 0.05				
$D_s^+ \to K_{1A}^0$				$D_s^+ \to K_{1B}^0$			
Model	$V_1(0)$	$V_2(0)$	$V_0(0)$	Model	$V_1(0)$	$V_2(0)$	$V_0(0)$
This work	0.51 ± 0.08	0.28 ± 0.03	-0.21 ± 0.05	This work	0.46 ± 0.07	0.23 ± 0.04	-0.17 ± 0.04
3PSR [33]	0.05	-0.02	0.03	3PSR [33]	-0.30	0.14	-0.26
LCSR [18]	0.28 ± 0.09	-0.01 ± 0.01	0.10 ± 0.04	LCSR [18]	-0.22 ± 0.09	0.24 ± 0.10	-0.41 ± 0.12
$D^+ \to \bar{K}_{1A}^0$				$D^+ \to \bar{K}_{1B}^0$			
Model	$V_1(0)$	$V_2(0)$	$V_0(0)$	Model	$V_1(0)$	$V_2(0)$	$V_0(0)$
This work	0.54 ± 0.09	0.37 ± 0.07	-0.33 ± 0.07	This work	0.48 ± 0.08	0.27 ± 0.04	-0.18 ± 0.04
3PSR [33]	0.02	-0.01	0.04	3PSR [33]	-0.16	0.08	-0.13
LCSR [18]	0.32 ± 0.11	-0.03 ± 0.01	0.11 ± 0.03	LCSR [18]	-0.26 ± 0.10	0.29 ± 0.13	-0.42 ± 0.14

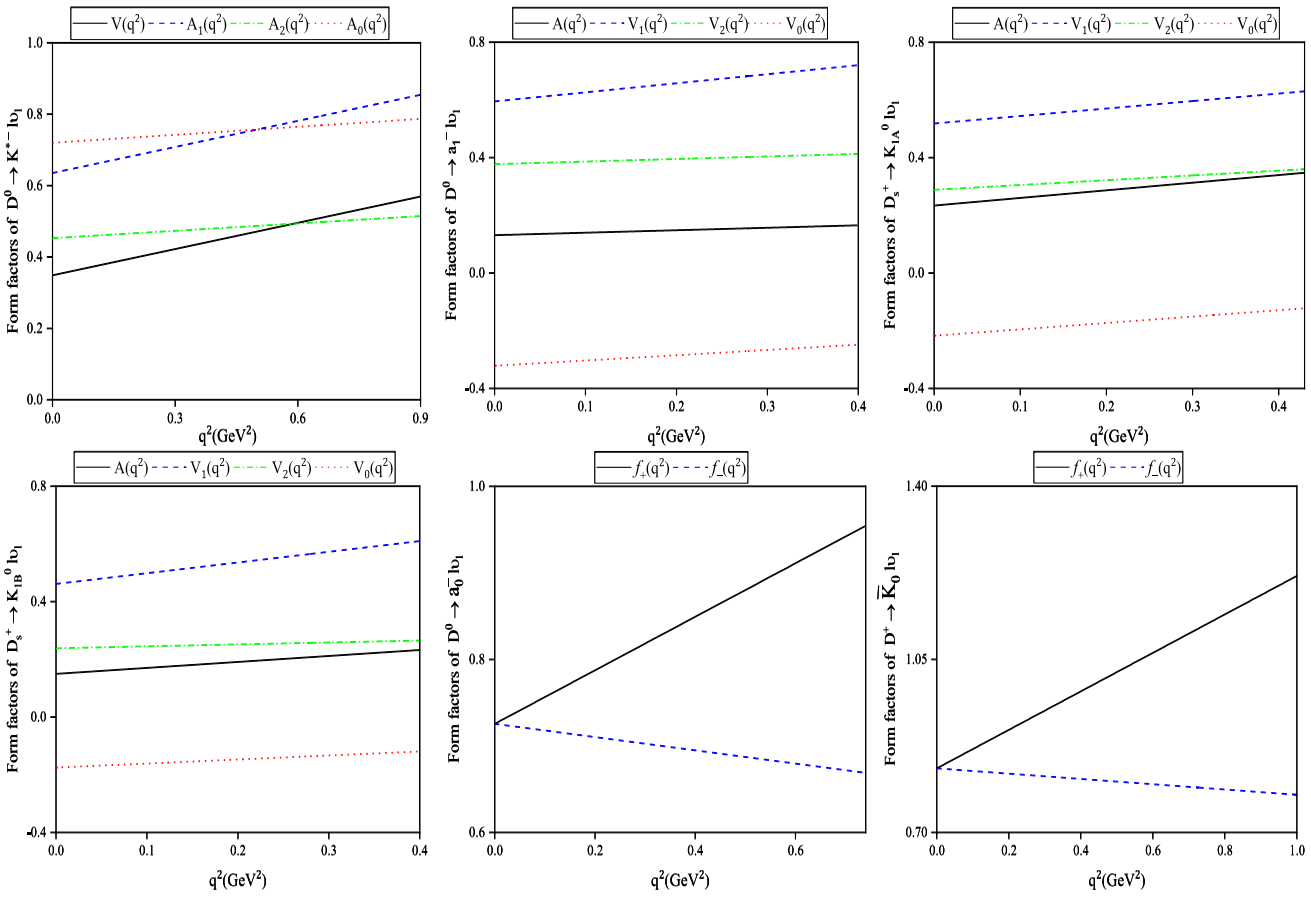

Fig. 2 Predictions for the q^2 dependence of six selected decays, $D^0 \to K^{*-}\,\ell\,\nu_\ell$, $D^0 \to a_1^-\,\ell\,\nu_\ell$, $D_s^+ \to K_{1A}^0\,\ell\,\nu_\ell$, $D_s^+ \to K_{1B}^0\,\ell\,\nu_\ell$, $D^0 \to a_0^-\,\ell\,\nu_\ell$ and $D^+ \to \bar{K}_0\,\ell\,\nu_\ell$

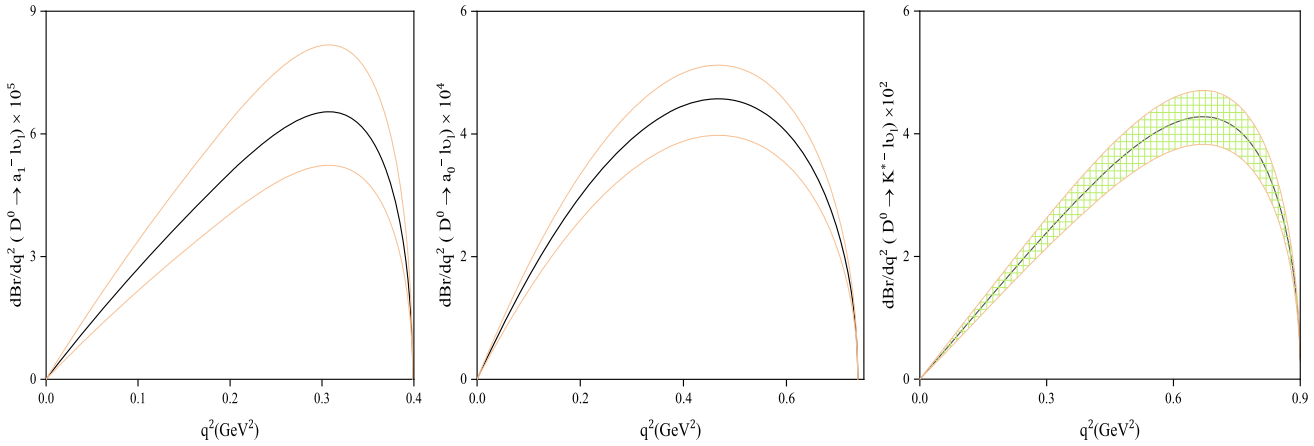

Fig. 3 Differential branching ratios of the $D^0 \to K^{*-}\,\ell\,\nu_\ell$, $D^0 \to a_1^-\,\ell\,\nu_\ell$ and $D^0 \to a_0^-\,\ell\,\nu_\ell$ as functions of q^2

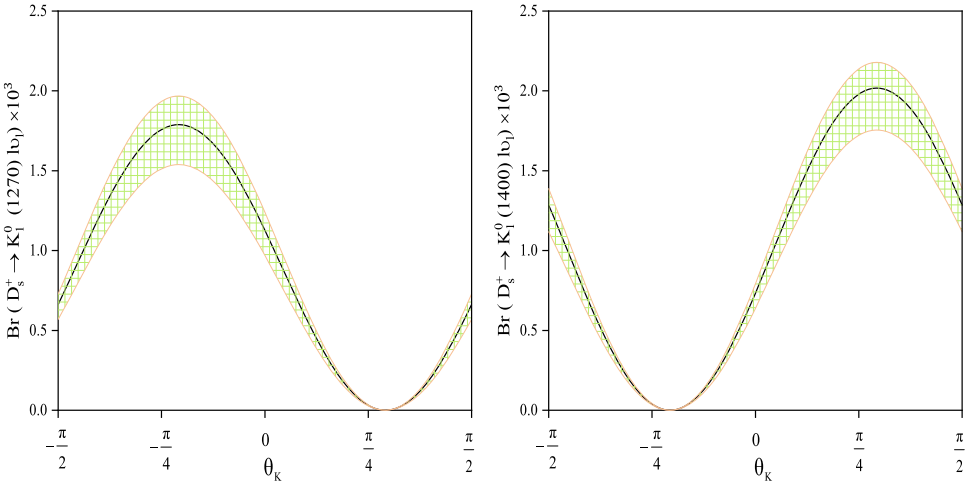

Fig. 4 The θ_K dependence of branching ratio values of $D_s^+ \to K_1^0(1270)\,\ell\,\nu_\ell$ and $D_s^+ \to K_1^0(1400)\,\ell\,\nu_\ell$ decays

Table 6 Branching ratios of the semileptonic decays $D \to V\,\ell\,\nu$. For comparison, we also present the results of other predictions

Model	Br $(D^0 \to \rho^-\ell\nu) \times 10^3$	Model	Br $(D^0 \to K^{*-}\ell\nu) \times 10^2$
This work	1.82 ± 0.15	This work	2.58 ± 0.26
LCSR [17]	$1.749^{+0.421}_{-0.297} \pm 0.006$		
CLEO (2013) [93]	$1.94 \pm 0.39 \pm 0.13$	Exp	2.15 ± 0.35
CLEO (2005) [98]	$1.77 \pm 0.12 \pm 0.10$		
3PSR [27]	0.5 ± 0.10	HMχT [91]	2.2
HQEFT [85]	1.40 ± 0.30		
NWA [99] + HQEFT [86]	1.67 ± 0.27	HQETF-I [85]	2.0 ± 0.5
NWA [99] + LFQM [90]	1.73 ± 0.07		
HMχT	2.00	HQETF-II [86]	2.12 ± 0.09

as follows:

$$\frac{d\Gamma}{dq^2}(D \to M\,\ell\,\nu_\ell) = \frac{G_F^2\,|V_{cq'}|^2\sqrt{\lambda}}{192\,m_D^3\pi^3}\,v^2\,q^2 \times (H_{1M}^2 + H_{2M}^2), \tag{73}$$

with

$$H_{1V} = (m_D + m_V)\,A_1(q^2) + m_D\,m_V\frac{2\,V(q^2)}{(m_D + m_V)}, \tag{74}$$

$$H_{2V} = \frac{1}{2\,m_V\sqrt{q^2}}\left[(m_D^2 - m_V^2 - q^2)\left((m_D + m_V)\,A_1(q^2) + m_D\,m_V\frac{2\,V(q^2)}{(m_D + m_V)}\right) - \frac{\lambda\,A_2(q^2)}{(m_D + m_V)}\right], \tag{75}$$

Table 7 Branching ratio values of the semileptonic $D \to A\,\ell\,\nu$ decays in Hard-Wall AdS/QCD, LCSR [18] and 3PSR [33,34]. For $D \to K_1\,\ell\,\nu$ with $K_1 = (K_1(1270), K_1(1400))$, the values of branching ratios are reported at $\theta_K = -(34 \pm 13)^\circ$

Process	This work	LCSR [18]	3PSR [34]	3PSR [33]	
$D^0 \to a_1^- \ell\nu$	$[1.42 \pm 0.35$	2.85 ± 0.41	$1.11^{+0.41}_{-0.34}$	–	$] \times 10^{-5}$
$D^0 \to b_1^- \ell\nu$	$[1.11 \pm 0.27$	1.88 ± 0.30	–	–	$] \times 10^{-5}$
$D_s^+ \to K_1^0(1270)$	$[1.75 \pm 0.15$	1.66 ± 0.05	–	1.25 ± 0.11	$] \times 10^{-3}$
$D_s^+ \to K_1^0(1400)$	$[0.14 \pm 0.02$	0.16 ± 0.02	–	0.14 ± 0.01	$] \times 10^{-3}$
$D^0 \to K_1^-(1270)$	$[5.27 \pm 0.30$	6.78 ± 0.12	–	5.34 ± 0.21	$] \times 10^{-3}$
$D^0 \to K_1^-(1400)$	$[0.71 \pm 0.03$	0.82 ± 0.05	–	0.85 ± 0.02	$] \times 10^{-3}$
$D^+ \to \bar{K}_1^0(1270)$	$[13.96 \pm 1.06$	16.86 ± 0.27	–	14.07 ± 1.22	$] \times 10^{-3}$
$D^+ \to \bar{K}_1^0(1400)$	$[1.25 \pm 0.12$	1.28 ± 0.08	–	1.27 ± 0.10	$] \times 10^{-3}$

Table 8 Branching ratios of $D \to S\,\ell\,\nu$ decays

Process	This work	LCSR [97]	CCQM [96]	
$D^0 \to a_0^- \ell\nu$	$[2.44 \pm 0.30$	$4.08^{+1.37}_{-1.22}$	1.68 ± 0.15	$] \times 10^{-4}$
$D_s^+ \to K_0 \ell\nu$	$[2.65 \pm 0.28$	–	–	$] \times 10^{-3}$
$D^0 \to K_0^- \ell\nu$	$[1.03 \pm 1.15$	–	–	$] \times 10^{-4}$
$D^+ \to \bar{K}^0 \ell\nu$	$[3.88 \pm 0.56$	–	–	$] \times 10^{-2}$

$$H_{1A} = (m_D - m_A)\,V_1(q^2) + m_D\,m_A\,\frac{2\,A(q^2)}{(m_D - m_A)}, \tag{76}$$

$$H_{2A} = \frac{1}{2\,m_A\sqrt{q^2}}\Bigg[(m_D^2 - m_A^2 - q^2)\Bigg((m_D - m_A)\,V_1(q^2) + m_D\,m_A\,\frac{2A(q^2)}{(m_D - m_A)}\Bigg) - \frac{\lambda\,V_2(q^2)}{(m_D - m_A)}\Bigg], \tag{77}$$

$$H_{1S} = (1 + \frac{m_\ell^2}{2\,q^2})^{\frac{1}{2}}\,\frac{2\,m_D\,\sqrt{\lambda}}{\sqrt{q^2}}\,f_+(q^2), \tag{78}$$

$$H_{2S} = \frac{1}{\sqrt{q^2}}(m_D^2 - m_S^2)\,f_-(q^2), \tag{79}$$

$$\nu = \left(1 - \frac{m_\ell^2}{q^2}\right),$$

$$\lambda = m_D^4 + m_M^4 + q^4 - 2\,m_D^2\,m_M^2 - 2\,m_D^2\,q^2 - 2\,m_M^2 q^2. \tag{80}$$

Note that the differences in the form factors $(A_3 - A_0)$ in $D \to V\,\ell\,\nu_\ell$ and $(V_3 - V_0)$ in $D \to A\,\ell\,\nu_\ell$ decays do not give any contribution, since these terms are proportional to m_ℓ^2 and can be ignored in our calculations for $\ell = e, \mu$. To calculate the branching ratio values of the semileptonic decays, we integrate Eq. (74) over q^2 in the whole physical region considering $|V_{cd(cs)}| = 0.22(0.97)$, and using the total mean life-times in ps as $\tau_{D^0} = 0.41$, $\tau_{D^+} = 1.04$, $\tau_{D_s^+} = 0.50$ [80]. The q^2 dependence of the differential branching ratios of 3 decay modes of the studied processes are plotted in Fig. 3. In this figure, $D^0 \to K^{*-}\,\ell\,\nu_\ell$, $D^0 \to a_1^-\,\ell\,\nu_\ell$ and $D^0 \to a_0^-\,\ell\,\nu_\ell$ are selected from D meson to vector, axial vector and scalar mesons decays, respectively and the uncertain regions, are also displayed. The branching ratios of $D_s^+ \to K_1^0(1270)\,\ell\,\nu_\ell$ and $D_s^+ \to K_1^0(1400)\,\ell\,\nu_\ell$ decay and their uncertain regions, are plotted as functions of the mixing angle θ_K in Fig. 4.

Predictions for the branching ratio values of the semileptonic decays $D \to (V, A, S)\ell\nu$ are presented in Tables 6, 7 and 8. For vector mesons as the final states, the predictions of LCSR [17], 3PSR [27], HQEFT [85], HMχT [91] and NWA [99] plus HQEFT [86] and plus LFQM [90], as well as the experimental measurements of CLEO Collaboration [93,98] are reported in Table 6. The LCSR [18] and 3PSR [33,34] predictions for $D \to A\ell\nu$ decays are also listed in Table 7. In this Table, the values are reported at $\theta_K = -(34 \pm 13)^\circ$ for the decays of charm mesons to $K_1(1270)$ and $K_1(1400)$. For decays of charm mesons to the scalar one, LCSR [97] and CCQM [96] models are utilized to evaluate the branching ratio of $D^0 \to a_0^-\ell\nu$ decay. The results of these calculations are itemized in Table 8.

5 Conclusion

In summary, the form factors of the semileptonic charm mesons decay into the light and strange vector, axial vector and scalar mesons are evaluated in Hard-Wall AdS/QCD including 4 flavours (u, d, s, c). The wave functions of the scalar mesons, the masses and the decay constants of this group are studied in detail, and our predictions for the masses

Table 9 The values of $M_V^{a\,2}$ and $M_A^{a\,2}$ with $v_q(z) = \zeta m_q z + \frac{1}{\zeta}\sigma_q z^3$ for $q = (u, d, s, c)$

a	$M_V^{a\,2}$	$M_A^{a\,2}$	a	$M_V^{a\,2}$	$M_A^{a\,2}$	a	$M_V^{a\,2}$	$M_A^{a\,2}$
(1, 2)	$\frac{1}{4}(v_u - v_d)^2$	$\frac{1}{4}(v_u + v_d)^2$	(6, 7)	$\frac{1}{4}(v_d - v_s)^2$	$\frac{1}{4}(v_d + v_s)^2$	(11, 12)	$\frac{1}{4}(v_d - v_c)^2$	$\frac{1}{4}(v_d + v_c)^2$
3	0	$\frac{1}{2}(v_u^2 + v_d^2)$	8	0	$\frac{1}{6}(v_u^2 + v_d^2 + 4v_s)^2$	(13, 14)	$\frac{1}{4}(v_c - v_s)^2$	$\frac{1}{4}(v_c + v_s)^2$
(4, 5)	$\frac{1}{4}(v_u - v_s)^2$	$\frac{1}{4}(v_u + v_s)^2$	(9, 10)	$\frac{1}{4}(v_u - v_c)^2$	$\frac{1}{4}(v_u + v_c)^2$	15	0	$\frac{1}{12}(v_u^2 + v_d^2 + v_s^2 + 9v_c^2)$

Table 10 The values of g^{abc}, h^{abc}, l^{abc} and k^{abc} which are used in numerical analysis

(a, b, c)	g^{abc}	h^{abc}	l^{abc}	k^{abc}
(2, 9, 11)	$\frac{1}{2}(v_u + v_d)(v_u + v_c)$	$\frac{1}{2}(v_u - v_d)(v_u + v_c)$	$\frac{1}{2}(v_d + v_c)(v_u + v_c)$	$\frac{1}{2}(v_d - v_u)(v_d + v_c)$
(4, 9, 13)	$\frac{1}{2}(v_u + v_s)(v_u + v_c)$	$\frac{1}{2}(v_u - v_s)(v_u + v_c)$	$\frac{1}{2}(v_s + v_c)(v_u + v_c)$	$\frac{1}{2}(v_u - v_s)(v_u + v_c)$
(6, 11, 13)	$-\frac{1}{2}(v_d + v_s)(v_s + v_c)$	$-\frac{1}{2}(v_s - v_d)(v_d + v_c)$	$\frac{1}{2}(v_d + v_c)(v_s + v_c)$	$\frac{1}{2}(v_c - v_s)(v_d + v_c)$

are compared with the experimental data. Moreover, the decay constants are compared with the results of the sum rule method.

Our estimations for the form factors at $q^2 = 0$ are compared with other theoretical frameworks such as: LCSR, 3PSR, HQETF, RHOPM, QM, LFQM, HMχT and LQCD, as well as the measurements of CLEO collaboration.

According to the presented definitions for the matrix elements in terms of form factors, the formulas for the decay widths are obtained. The branching ratios are estimated for the mentioned model and the results are compared with the experimental data and the predictions of the other theoretical approaches. The prediction for the branching ratio of the $D^0 \to \rho^- \ell \nu$ decay is in good agreement with the reported results of LCSR, HQEFT, LFQM, and the experimental values. For the semileptonic $D^0 \to K^{*-} \ell \nu$ decay, the estimation for the branching ratio value has a better agreement with the experimental report. The predicted form factors in this study can be used to evaluate the branching fraction of nonleptonic and forward–backward asymmetry of leptonic D meson decays. This model can also be extended to 5 flavours with $q = (u, d, s, c, b)$ to study the B meson decays.

Data Availability Statement This manuscript has no associated data or the data will not be deposited. [Authors' comment: In Table 6, the results of experimental data from CLEO(2013) [93] and CLEO(2005) [98] are considered and compared with the obtained theoretical results in this work.]

Funded by SCOAP[3].

Appendix: Values of $M_V^{a\,2}$, $M_A^{a\,2}$, g^{abc}, h^{abc}, l^{abc} and k^{abc}

Table 9 [68] represents the values of $M_V^{a\,2}$ and $M_A^{a\,2}$, which are used to evaluate the wave functions.

The nonzero values for g^{abc}, h^{abc}, l^{abc} and k^{abc} used in numerical analysis are given in Table 10.

References

1. M. Ablikim et al. (BESIII Collaboration), Phys. Rev. D **96**, 012002 (2017)
2. M. Ablikim et al. (BESIII Collaboration), Phys. Rev. Lett. **121**, 171803 (2018)
3. M. Ablikim et al. (BESIII Collaboration), Phys. Rev. D **97**, 012006 (2018)
4. M. Ablikim et al. (BESIII Collaboration), Phys. Rev. D **97**, 092009 (2018)
5. M. Ablikim et al. (BESIII Collaboration), Phys. Rev. Lett. **122**, 011804 (2019)
6. M. Ablikim et al. (BESIII Collaboration), Phys. Rev. Lett. **122**, 121801 (2019)
7. M. Ablikim et al. (BESIII Collaboration), Phys. Rev. Lett. **122**, 061801 (2019)
8. M. Ablikim et al. (BESIII Collaboration), Phys. Rev. D **99**, 011103 (2019)
9. M. Ablikim et al. (BESIII Collaboration) Phys. Rev. Lett. **122**, 062001 (2019)
10. A. Zupanc et al. (BESIII Collaboration), JHEP **09**, 139 (2013)
11. A. J. Schwartz, arXiv: 1902.07850 [hep-ex]
12. L. Widhalm et al. (Belle Collaboration) Phy. Rew. Lett **97**, 061804 (2006)
13. N.R. Soni, J.N. Pandya, Phys. Rev. D **96**, 016017 (2017)
14. N. R. Soni, M. A. Ivanov, J. G. Korner, J. N. Pandya, P. Santorelli, C. T. Tran, arXiv: 1810.11907 [hep-ph]
15. A. Khodjamirian, R. Ruckl, S. Weinzierl, C. Winhart, O.I. Yakovlev, Phys. Rev. D **62**, 114002 (2000)

16. P. Ball, Phys. Lett. B **641**, 50 (2006)
17. H.B. Fu, X. Yang, R. Lü, L. Zeng, W. Cheng, X.G. Wu, Eur. Phys. J. C **80**, 194 (2020)
18. S. Momeni, R. Khosravi, J. Phys. G: Nucl. Part. Phys. **46**, 105006 (2019)
19. J. Zhang, C.X. Yue, C.H. Li, Eur. Phys. J. C **78**, 695 (2018)
20. W.Y. Wang, Y.L. Wu, M. Zhong, Phys. Rev. D **67**, 014024 (2003)
21. A. Abada et al. (SPQcdR collaboration) Nucl. Phys. Proc. Suppl. **119**, 625 (2003)
22. C. Aubin et al. (Fermilab Lattice) Phys. Rev. Lett. **94**, 011601 (2005)
23. C. Bernard et al., Phys. Rev. D **80**, 034026 (2009)
24. I. Bediaga, M. Nielsen, Phys. Rev. D **68**, 036001 (2003)
25. T.M. Aliev, V.L. Eletsky, Ya.. I. Kogan, Sov. J. Nucl. Phys. **40**, 527 (1984)
26. P. Ball, V.M. Braun, H.G. Dosch, Phys. Rev. D **44**, 3567 (1991)
27. P. Ball, Phys. Rev. D **48**, 3190 (1993)
28. A.A. Ovchinnikov, V.A. Slobodenyuk, Z. Phys. C **44**, 433 (1989)
29. V.N. Baier, A. Grozin, Z. Phys. C **47**, 669 (1990)
30. D.S. Du, J.W. Li, M.Z. Yang, Eur. Phys. J. C **37**, 137 (2004)
31. M.Z. Yang, Phys. Rev. D **73**, 034027 (2006)
32. M.Z. Yang, Phys. Rev. D **73**, 079901(E) (2006)
33. R. Khosravi, K. Azizi, N. Ghahramany, Phys. Rev. D **79**, 036004 (2009)
34. Y. Zuo et al., Int. J. Mod. Phys. A **31**, 1650116 (2016)
35. J.M. Maldacena, Adv. Theor. Math. Phys. **2**, 231 (1998)
36. E. Witten, Adv. Theor. Math. Phys. **2**, 253 (1998)
37. S.S. Gubser, I.R. Klebanov, A.M. Polyakov, Phys. Lett. B **428**, 105 (1998)
38. G.P. Lepage, S.J. Brodsky, Phys. Rev. D **22**, 2157 (1980)
39. G.F. de Teramond, S.J. Brodsky, Phys. Rev. Lett. **102**, 081601 (2009)
40. A. Karch, E. Katz, D.T. Son, M.A. Stephanov, Phys. Rev. D **74**, 015005 (2006)
41. S. J. Brodsky, G. F. de Teramond, arXiv: 0802.0514 [hep-ph]
42. S.J. Brodsky, G.F. de Teramond, Word Sci. Subnuclear Ser. **45**, 139 (2009)
43. S.J. Brodsky, G.F. de Teramond, Phys. Rev. D **77**, 056007 (2008)
44. J.R. Forshaw, R. Sandapen, J. High Energy Phys. **10**, 093 (2011)
45. M. Ahmady, R. Sandapen, Phys. Rev. D **87**, 054013 (2013)
46. M. Ahmady, R. Sandapen, Phys. Rev. D **88**, 014042 (2013)
47. M. Ahmady, R. Campbell, S. Lord, R. Sandapen, Phys. Rev. D **88**, 074031 (2013)
48. M. Ahmady, R. Campbell, S. Lord, R. Sandapen, Phys. Rev. D **88**, 014042 (2014)
49. M.R. Ahmady, S. Lord, R. Sandapen, Phys. Rev. D **90**, 074010 (2014)
50. M. Ahmady, S. Lord, R. Sandapen, Nucl. Part. Phys. Proc. **273–275** (2016)
51. Q. Chang, S.J. Brodsky, X.Q. Li, Phys. Rev. D **95**, 094025 (2017)
52. S. Momeni, R. Khosravi, Phys. Rev. D **95**, 016009 (2017)
53. S. Momeni, R. Khosravi, Eur. Phys. J. C **78**, 805 (2018)
54. M. Ahmady, C. Mondal, R. Sandapen, Phys. Rev. D **100**, 054005 (2019)
55. M. Ahmady, S. Kaur, C. Mondal, R. Sandapen, Phys. Rev. D **102**, 034021 (2020)
56. J. Polchinski, M.J. Strassler, Phys. Rev. Lett. **88**, 031601 (2002)
57. J. Polchinski, M.J. Strassler, JHEP **05**, 012 (2003)
58. H.R. Grigoryan, A.V. Radyushkin, Phys. Rev. D **76**, 095007 (2007)
59. H.R. Grigoryan, A.V. Radyushkin, Phys. Rev. D **76**, 115007 (2007)
60. H.R. Grigoryan, A.V. Radyushkin, Phys. Rev. D **78**, 115008 (2008)
61. H.J. Kwee, R.F. Lebed, JHEP **01**, 027 (2008)
62. H.J. Kwee, R.F. Lebed, Phys. Rev. D **77**, 115007 (2008)
63. H. Boschi-Filho, N.R.F. Braga, H.L. Carrion, Phys. Rev. D **73**, 047901 (2006)
64. Z. Abidin, C.E. Carlson, Phys. Rev. D **78**, 071502 (2008)
65. Z. Abidin, C.E. Carlson, Phys. Rev. D **79**, 115003 (2009)
66. Z. Abidin, C.E. Carlson, Phys. Rev. D **80**, 115010 (2009)
67. A.B. Bayona, G. Krein, C. Miller, Phys. Rev. D **96**, 014017 (2017)
68. S. Momeni, M. Saghebfar, Eur. Phys. J. C **81**, 102 (2021)
69. J. Erlich, E. Katz, D.T. Son, M.A. Stephanov, Phys. Rev. Lett. **95**, 261602 (2005)
70. A. Cherman, T.D. Cohen, E.S. Werbos, Phys. Rev. C **79**, 045203 (2009)
71. E. Katz, M.D. Schwartz, JHEP **08**, 077 (2007)
72. J.P. Shock, F. Wu, JHEP **08**, 023 (2006)
73. L. Burakovsky, T. Goldman, Phys. Rev. D **57**, 2879 (1998)
74. M. Suzuki, Phys. Rev. D **47**, 1252 (1993)
75. H. Hatanaka, K.C. Yang, Phys. Rev. D **77**, 094023 (2008)
76. H.R. Grigoryan, A.V. Radyushkin, Phys. Lett. B **650**, 421 (2007)
77. Z. Abidin, C.E. Carlson, Phys. Rev. D **77**, 095007 (2008)
78. M.A.A. Sbaih, M.K.H. Srour, M.S. Hamada, H.M. Fayad, Electron. J. Theor. Phys. **28**, 9 (2013)
79. Z. Abidin, C.E. Carlson, Phys. Rev. D **77**, 115021 (2008)
80. P.A. Zyla et al. (Particle Data Group), Prog. Theor. Exp. Phys. 083C01 (2020)
81. K. Maltman, Phys. Lett. B **462**, 14 (1999)
82. J.Y. Sungu, H. Sundu, K. Azizi, N. Yinelek, S. Sahin, Proceedings of Science, Poster Presentation, The Many Faces of QCD, Gent, Belgium, (2010)
83. H. Cheng, Phys. Rev. D **67**, 034024 (2003)
84. K. Yang, Nucl. Phys. B **776**, 187 (2007)
85. W.Y. Wang, Y.L. Wu, M. Zhong, Phys. Rev. D **67**, 014024 (2003)
86. Y.L. Wu, M. Zhong, Y.B. Zuo, Int. J. Mod. Phys. A **21**, 6125 (2006)
87. M. Wirbel, B. Stech, M. Bauer, Z. Phys. C **29**, 637 (1985)
88. N. Isgur, D. Scora, B. Grinstein, M.B. Wise, Phys. Rev. D **39**, 799 (1989)
89. D. Melikhov, B. Stech, Phys. Rev. D **62**, 014006 (2000)
90. R.C. Verma, J. Phys. G **39**, 025005 (2012)
91. S. Fajfer, J.F. Kamenik, Phys. Rev. D **72**, 034029 (2005)
92. C.W. Bernard, A.X. El-Khadra, A. Soni, Phys. Rev. D **45**, 869 (1992)
93. S. Dobbs et al. (CLEO Collaboration) Phys. Rev. Lett. **110**, 131802 (2013)
94. H.Y. Cheng, C.K. Chua, C.W. Hwang, Phys. Rev. D **69**, 074025 (2004)
95. P. Ball, V.M. Braun, Phys. Rev. D **58**, 094016 (1998)
96. N.R. Soni, A.N. Gadaria, J.J. Patel, J.N. Pandya, Phys. Rev. D **102**, 016013 (2020)
97. X.-D. Cheng, H.-B. Li, B. Wei, Y.-G. Xu, M.-Z. Yang, Phys. Rev. D **96**, 033002 (2017)
98. G.S. Huang et al. (CLEO Collaboration) Phys. Rev. Lett. **95**, 181801 (2005)
99. Y.J. Shi, W. Wang, S. Zhao, Eur. Phys. J. C **77**, 452 (2017)